knockdown of PKC reduced Akt phosphorylation at Ser473 and increased the level of $p21^{Cip1}$ [23]; these observations are consistent with our data. We found that sangivamycin suppressed the phosphorylation of Erk and Akt, thus inhibiting Erk and Akt signaling, which is necessary for the survival of PEL cells. Such inhibition by sangivamycin may cause the apoptosis of PEL cells.

3.4. Low levels of sangivamycin with GA or valproate suppress the proliferation of PEL cells

Previously, we reported that the HSP90 inhibitor geldanamycin (GA) induced apoptosis in PEL cells by inhibiting NF-κB signaling [17,19]. Valproate (valproic acid) also induces the apoptosis of PEL cells, accompanied by KSHV re-activation [24]. It is well known that combined therapies for lymphoma are more effective than monotherapies. Therefore, we investigated whether treatment with a low concentration of sangivamycin in combination with GA or valproate (also at low levels) inhibited the proliferation of BCBL1 cells. Such cells were treated with 25 nM sangivamycin alone, 10 nM GA alone (Fig. 4A), 0.5 mM valprolate alone (Fig. 4B), a combination of 25 nM sangivamycin and 10 nM GA (Fig. 4A), or a combination of 25 nM sangivamycin and 0.5 mM valprolate (Fig. 4B). Cell viability was measured after 1, 2, or 3 days. Sangivamycin, GA, or valproate alone did not inhibit the growth of BCBL1 cells. However, the combination of 25 nM sangivamycin with 10 nM GA or 25 nM sangivamycin with 0.5 mM valproate suppressed the proliferation of BCBL1 cells in a synergistic manner. Such drug mixtures are thus novel strategies for the treatment of PEL. The HSP90 inhibitor GA induces apoptosis in PEL cells by stabilizing IκBα, which in turn suppresses NF-κB signaling [19]. Constitutive activation of NF-κB signaling is essential for the survival of PEL cells. HSP90 functions as a scaffold for the IKK complex, and thus contributes to upregulation of NF-κB activity by destabilizing IκB. We found that the inhibition of NF-κB and Erk signaling by GA and sangivamycin strongly compromised the survival of PEL cells, indicating that co-activation of NF-κB and Erk may be important in this context. Valproate is clinically used as an anti-epileptic drug and a mood stabilizer. Additionally, valproate functions as an inhibitor of histone deacetylases and induces the apoptosis of transformed cells, including PEL and EBV-infected lymphoma cells [24]. These findings, and our present data, suggest that histone deacetylation as well as signaling by NF-κB and Erk enhance the survival of PEL cells.

Finally, we examined the effects of sangivamycin on lytic replication in PEL cells. The addition of *n*-butyrate induces viral replication in KSHV-infected BCBL1 cells. As treatment with 25 nM sangivamycin remarkably reduced the viability of BCBL1 cells, such cells were treated with 0.5–10 nM sangivamycin in the presence or absence of 1.5 mM *n*-butyrate for 24 h. Sangivamycin did not induce KSHV lytic replication in BCBL1 cells that were not treated with *n*-butyrate (Fig. 4C). Further, sangivamycin did not affect the level of virus production in *n*-butyrate-treated BCBL1

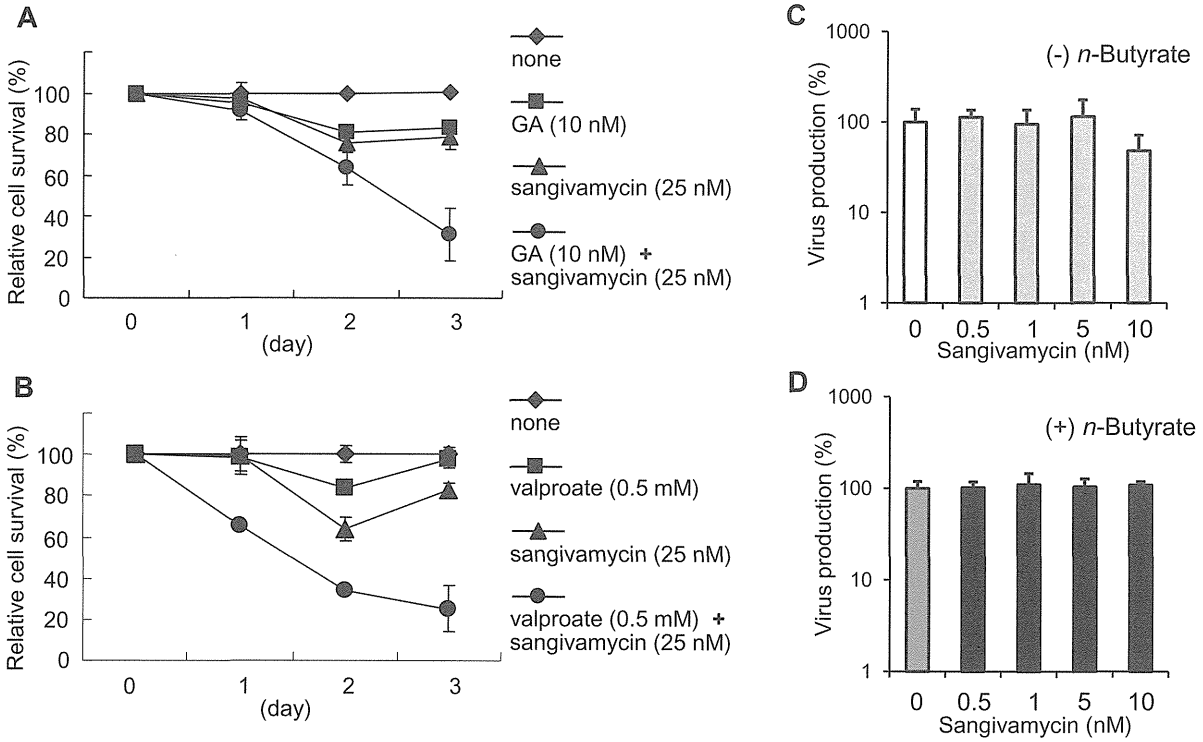

Fig. 4. Enhancement of the cytotoxic effects of geldanamycin (GA) or valproate by sangivamycin. (A) The cytotoxic effects of GA alone, sangivamycin alone, or a combination of sangivamycin and GA, on BCBL1 cells. (B) The cytotoxic effects of valproate alone, sangivamycin alone, or a combination of sangivamycin and valproate, on BCBL1 cells. Cells were treated with 25 nM sangivamycin, 10 nM GA, 0.5 mM valprolate, a combination of 25 nM sangivamycin and 10 nM GA, or a combination of 25 nM sangivamycin and 0.5 mM valproate, and cell viability was measured after 1, 2, and 3 days. The viability of untreated cells was defined to be 100%. (C) The effect of sangivamycin on lytic induction in BCBL1 cells not treated with *n*-butyrate. The cells were treated with sangivamycin for 24 h, and culture medium containing virus particles was harvested. The KSHV genome levels were quantified via real-time PCR. The KSHV genome copy number in sangivamycin-untreated BCBL1 cells was defined to be 100%. (D) Effects of sangivamycin on lytic replication in BCBL1 cells treated with *n*-butyrate. BCBL1 cells were treated with sangivamycin in the presence of 1.5 mM *n*-butyrate for 24 h to induce lytic replication. KSHV genomes were purified from the culture medium and quantified via real-time PCR. The KSHV genome copy number in medium from sangivamycin-untreated cells was defined to be 100%.

cells, in which lytic replication was induced (Fig. 4D). Fig. 3A shows that sangivamycin did not induce lytic replication in either BCBL1 or BC3 cells. Sangivamycin did not induce K-bZIP expression, which is induced during lytic replication. Together, our data show that sangivamycin induces apoptosis in PEL cells without production of progeny virus; thus, sangivamycin may serve as a useful treatment for PEL without any risk of *de novo* KSHV infection.

Acknowledgments

This work was partly supported by a Health and Labor Sciences Research Grant (no. H23-AIDS-Ippan-002) from the Ministry of Health, Labor, and Welfare of Japan; a Grant-in-Aid for Scientific Research (C) from the Ministry of Education, Culture, Sports, Science and Technology, Japan (KAKENHI 24590103); and the Project of Establishing Medical Research Base Networks against Infectious Diseases in Okinawa.

References

[1] D.E. Bergstrom, A.J. Brattesani, M.K. Ogawa, P.A. Reddy, M.J. Schweickert, J. Balzarini, E. De Clercq, Antiviral activity of C-5 substituted tubercidin analogues, J. Med. Chem. 27 (1984) 285–292.
[2] S.R. Turk, C. Shipman Jr., R. Nassiri, G. Genzlinger, S.H. Krawczyk, L.B. Townsend, J.C. Drach, Pyrrolo[2,3-d]pyrimidine nucleosides as inhibitors of human cytomegalovirus, Antimicrob. Agents Chemother. 31 (1987) 544–550.
[3] P.S. Ritch, R.I. Glazer, R.E. Cunningham, S.E. Shackney, Kinetic effects of sangivamycin in sarcoma 180 in vitro, Cancer Res. 41 (1981) 1784–1788.
[4] S.A. Lee, M. Jung, The nucleoside analog sangivamycin induces apoptotic cell death in breast carcinoma MCF7/adriamycin-resistant cells via protein kinase Cdelta and JNK activation, J. Biol. Chem. 282 (2007) 15271–15283.
[5] M.B. Cohen, R.I. Glazer, Comparison of the cellular and RNA-dependent effects of sangivamycin and toyocamycin in human colon carcinoma cells, Mol. Pharmacol. 27 (1985) 349–355.
[6] C.R. Loomis, R.M. Bell, Sangivamycin, a nucleoside analogue, is a potent inhibitor of protein kinase C, J. Biol. Chem. 263 (1988) 1682–1692.
[7] M.K. Kim, Y.H. Cho, J.M. Kim, M.W. Chun, S.K. Lee, Y. Lim, C.H. Lee, Induction of apoptosis in human leukemia cells by MCS-C2 via caspase-dependent Bid cleavage and cytochrome c release, Cancer Lett. 223 (2005) 239–247.
[8] J.J. Russo, R.A. Bohenzky, M.C. Chien, J. Chen, M. Yan, D. Maddalena, J.P. Parry, D. Peruzzi, I.S. Edelman, Y. Chang, P.S. Moore, Nucleotide sequence of the Kaposi sarcoma-associated herpesvirus (HHV8), Proc. Natl. Acad. Sci. U. S. A. 93 (1996) 14862–14867.
[9] R.G. Nador, E. Cesarman, A. Chadburn, D.B. Dawson, M.Q. Ansari, J. Sald, D.M. Knowles, Primary effusion lymphoma: a distinct clinicopathologic entity associated with the Kaposi's sarcoma-associated herpes virus, Blood 88 (1996) 645–656.
[10] Y. Chang, E. Cesarman, M.S. Pessin, F. Lee, J. Culpepper, D.M. Knowles, P.S. Moore, Identification of herpesvirus-like DNA sequences in AIDS-associated Kaposis sarcoma, Science 266 (1994) 1865–1869.
[11] A. Järviluoma, P.M. Ojala, Cell signaling pathways engaged by KSHV, Biochim. Biophys. Acta 1766 (2006) 140–158.
[12] M. Fujimuro, F.Y. Wu, C. apRhys, H. Kajumbula, D.B. Young, G.S. Hayward, S.D. Hayward, A novel viral mechanism for dysregulation of β-catenin in Kaposis sarcoma-associated herpesvirus latency, Nat. Med. 9 (2003) 300–306.
[13] A. Ashizawa, C. Higashi, K. Masuda, R. Ohga, T. Taira, M. Fujimuro, The Ubiquitin System and Kaposi's sarcoma-associated herpesvirus, Front. Microbiol. 3 (2012) 66.
[14] P.P. Naranatt, S.M. Akula, C.A. Zien, H.H. Krishnan, B. Chandran, Kaposi's sarcoma-associated herpesvirus induces the phosphatidylinositol 3-kinase-PKC-zeta-MEK-ERK signaling pathway in target cells early during infection: implications for infectivity, J. Virol. 77 (2003) 1524–1539.
[15] M.J. Smit, D. Verzijl, P. Casarosa, M. Navis, H. Timmerman, R. Leurs, Kaposi's sarcoma-associated herpesvirus-encoded G protein-coupled receptor ORF74 constitutively activates p44/p42 MAPK and Akt via G(i) and phospholipase C-dependent signaling pathways, J. Virol. 76 (2002) 1744–1752.
[16] A. Cohen, C. Brodie, R. Sarid, An essential role of ERK signaling in TPA-induced reactivation of Kaposi's sarcoma-associated herpesvirus, J. Gen. Virol. 87 (2006) 795–802.
[17] C. Saji, C. Higashi, Y. Niinaka, K. Yamada, K. Noguchi, M. Fujimuro, Proteasome inhibitors induce apoptosis and reduce viral replication in primary effusion lymphoma cells, Biochem. Biophys. Res. Commun. 415 (2011) 573–578.
[18] M. Fujimuro, J. Liu, J. Zhu, H. Yokosawa, S.D. Hayward, Regulation of the interaction between glycogen synthase kinase 3 and the Kaposi's sarcoma-associated herpesvirus latency-associated nuclear antigen, J. Virol. 79 (2005) 10429–10441.
[19] C. Higashi, C. Saji, K. Yamada, H. Kagawa, R. Ohga, T. Taira, M. Fujimuro, The effects of heat shock protein 90 inhibitors on apoptosis and viral replication in primary effusion lymphoma cells, Biol. Pharm. Bull. 35 (2012) 725–730.
[20] P.M. Chaudhary, A. Jasmin, M.T. Eby, L. Hood, Modulation of the NF-κ B pathway by virally encoded death effector domains-containing proteins, Oncogene 18 (1999) 5738–5746.
[21] T.J. Nelson, M.K. Sun, J. Hongpaisan, D.L. Alkon, Insulin, PKC signaling pathways and synaptic remodeling during memory storage and neuronal repair, Eur. J. Pharmacol. 585 (2008) 76–87.
[22] S. Montaner, A. Sodhi, S. Pece, E.A. Mesri, J.S. Gutkind, The Kaposi's sarcoma-associated herpesvirus G protein-coupled receptor promotes endothelial cell survival through the activation of Akt/protein kinase B, Cancer Res. 61 (2001) 2641–2648.
[23] J.M. Haughian, E.M. Reno, A.M. Thorne, A.P. Bradford, Protein kinase C alpha-dependent signaling mediates endometrial cancer cell growth and tumorigenesis, Int. J. Cancer 125 (2009) 2556–2564.
[24] C.M. Klass, L.T. Krug, V.P. Pozharskaya, M.K. Offermann, The targeting of primary effusion lymphoma cells for apoptosis by inducing lytic replication of human herpesvirus 8 while blocking virus production, Blood 105 (2005) 4028–4034.

Virology 425 (2012) 95–102

Contents lists available at SciVerse ScienceDirect

Virology

journal homepage: www.elsevier.com/locate/yviro

Novel monoclonal antibodies for identification of multicentric Castleman's disease; Kaposi's sarcoma-associated herpesvirus-encoded vMIP-I and vMIP-II

Kazushi Nakano [a,1], Harutaka Katano [c,1], Kenjiro Tadagaki [b], Yuko Sato [c], Eriko Ohsaki [a], Yasuko Mori [d,e], Koichi Yamanishi [e], Keiji Ueda [a,*]

[a] Division of Virology, Department of Microbiology and Immunology, Osaka University Graduate School of Medicine, 2-2 Yamada-oka, Suita, Osaka 565-0871, Japan
[b] Institut Cochin, Université Paris Descartes, CNRS (UMR 8104) Inserm U1016, Paris, France
[c] Department of Pathology, National Institute of Infectious Diseases, Tokyo, Japan
[d] Division of Clinical Virology, Kobe University Graduate School of Medicine, 7-5-1, Kusunoki-cho, Chuo-ku, Kobe, 650-0017, Japan
[e] Division of Biomedical Research, National Institute of Biomedical Innovation, Ibaraki, Osaka, Japan

ARTICLE INFO

Article history:
Received 29 August 2011
Returned to author for revision 2 October 2011
Accepted 11 January 2012
Available online 31 January 2012

Keywords:
Kaposi's sarcoma-associated herpesvirus
Kaposi's sarcoma
Multicentric Castleman's disease
Viral macrophage inflammatory protein
vMIP-I
vMIP-II
Chemokine
KSHV
HHV-8

ABSTRACT

Recent studies have indicated that vMIP-I and vMIP-II play important roles in the pathogenesis of Kaposi's sarcoma-associated herpesvirus (KSHV)-related diseases due to the effects of these proteins on vascularization. We developed monoclonal antibodies against KSHV-encoded viral macrophage inflammatory protein-I (vMIP-I) and vMIP-II to study these expression profiles and reveal the pathogenesis of KSHV-related diseases. The MAbs against vMIP-I and vMIP-II reacted to KSHV-infected cell lines after lytic induction. Both vMIP-I and the vMIP-II gene products were detected 24 h post-induction with 12-*O*-tetradecanoylphorbol-13-acetate until 60 h in the cytoplasm of primary effusion lymphoma cell lines. In clinical specimens, both vMIP-I and vMIP-II gene products were detected in the tissues of patients with multicentric Castleman's disease. On the other hand, only vMIP-II was detected in a subset of Kaposi's sarcoma. We concluded that these antibodies might be powerful tools to elucidate the pathogenesis of KSHV-related diseases.

Introduction

Kaposi's sarcoma-associated herpesvirus (KSHV), also known as human herpesvirus 8 (HHV-8), is a gammaherpesvirus originally identified in HIV-positive Kaposi's sarcoma (KS) tissues (Chang et al., 1994). KSHV is responsible for AIDS associated cancers such as Kaposi's sarcoma (KS), primary effusion lymphoma (PEL), and multicentric Castleman's disease (MCD) (Cesarman et al., 1995; Schalling et al., 1995; Soulier et al., 1995). As is the case for all herpesviruses, KSHV has two life cycles, one latent and the other lytic. Lytic gene expression can be induced by the treatment of latently infected cells with chemical agents such as 12-*O*-tetradecanoylphorbol-13-acetate (TPA), sodium butyrate (Arvanitakis et al., 1996; Miller et al., 1997). It has been demonstrated that two KSHV-encoded chemokines, K6 (which encodes a vMIP-I) and K4 (which encodes a vMIP-II), are expressed in the course of lytic infection (Moore et al., 1996; Sun et al., 1999). Previous reports showed that both vMIP-I and vMIP-II induced Ca^{2+} signal transduction via certain chemokine receptors and the receptor-dependent migration of cells (Benelli et al., 2000; Chen et al., 1998; Endres et al., 1999; Kledal et al., 1997). In addition, in a chick chorioallantoic membrane assay, the both proteins showed strong angiogenic properties (Boshoff et al., 1997). However, little is known about the contribution of vMIPs to KSHV malignancy under physiologic conditions.

In this report, we generated new monoclonal antibodies against vMIP-I and vMIP-II, and confirmed the detection of both vMIP-I and vMIP-II in histological sections of tissues from MCD patients as well as in KSHV-infected PEL cell lines. In cases of KS, vMIP-II was detected, but not vMIP-I. These results suggest that the expression properties of vMIP-I and vMIP-II might be related to KSHV-associated diseases, and may even be involved in the generation of diseases. Thus, antiviral chemokine MAbs could potentially become useful tools for the diagnosis of KSHV-related diseases.

Materials and methods

Cells

Kaposi's sarcoma-associated herpesvirus-positive cell lines (BC-1, BC-3, BCBL-1 and TY-1 cells) and a negative cell line (BJAB cells) were

* Corresponding author. Tel.: +81 6 6879 3780; fax: +81 6 6879 3789.
E-mail address: kueda@virus.med.osaka-u.ac.jp (K. Ueda).
[1] Equal contribution by these authors.

0042-6822/$ – see front matter © 2012 Elsevier Inc. All rights reserved.
doi:10.1016/j.virol.2012.01.008

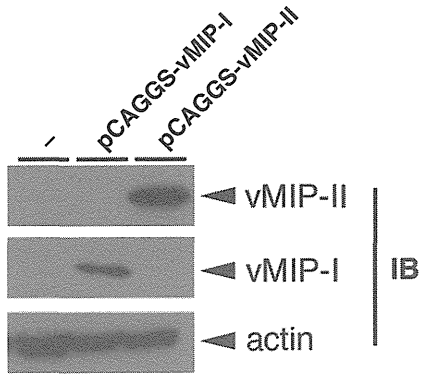

Fig. 1. Cross reactivity between anti-vMIP-I and anti-vMIP-II MAb. 293 T cells were transfected with either 2 μg of pCAGGS- vMIP-I or 2 μg of pCAGGS-vMIP-II plasmids. Forty-eight hours after transfection, the cells were harvested and expression of vMIP-I or vMIP-II was tested by Western blot analysis using the anti-vMIP-I or -vMIP-II MAb, respectively. Actin was also probed with anti-actin monoclonal Ab as a loading control.

obtained from the American Type Culture Collection (ATCC) (Manassas, VA). These cells were grown in RPMI 1640 (Nakalai Tesque, Inc., Kyoto, Japan) supplemented with 10 IU/ml penicillin G, 10 μg/ml streptomycin, 10% heat-inactivated fetal bovine serum (FBS) (HyClone, Logan, UT) in a 5% CO_2 atmosphere. In addition, 293 T and 293/EBNA (Clontech) cells were grown in Dulbecco's modified Eagle's medium (DMEM) (Nakalai Tesque, Inc.) supplemented with 10 IU/ml penicillin G, and 10 μg/ml streptomycin, 10% FBS, and 200 mM L-glutamine.

Plasmids

In order to express vMIP-I and vMIP-II, the ORFs were cloned into the pCAGGS eukaryotic expression vector, and pCAGGS-vMIP-I and pCAGGS-vMIP-II were established. The plasmid vector, pCAGGS was kindly provided by Dr. J. Miyazaki of Osaka University (Niwa et al., 1991). Briefly, fragments including vMIP-I and vMIP-II ORFs were amplified by PCR using the following primer sets: vMIP-I-Met (5′-CGGTACCGAATTCTCCAGATGGCC-3′) and vMIP-I-Ter (5′-ACTCGA-GAATTCTACTTGTCATCGTCGTCCTTGTAGTCGGAAGCTATGGCAGGCAG-3′); and vMIP-II-Met (5′-AGGTACCGAATTCAGTTATGGACACCAAGGGC-3′) and vMIP-II-Ter (5′-ACTCGAGAATTCTACTTGTCATCGTCGTCCTTG-TAGTCGGAGCGAGCAGTGACTGG-3′). The PCR products were cloned into pCR2.1 (Invitrogen) and sequenced. After digestion with *Eco*RI, the fragments were ligated into the *Eco*RI site of the pCAGGS vector. Then, the DNA fragments encoding vMIP-I and vMIP-II were liberated by *Eco*RI, and were inserted into pCAGGS to generate the expression vectors pCAGGS-vMIP-I and -vMIP-II, respectively. vMIP-I (pGEX-vMIP-I) and vMIP-II (pGEX-vMIP-II) were also generated using PCR-based technology using BCBL-1 genomic DNA as a templete. The coding region, without a signal peptide, was amplified with vMIP-I-Eco (CAGAATTCGCGGGGTCACTCGTGTCG-3′), vMIP-I-Sal (CTGTCGACCGTC-TAAGCTATGGCAGG-3′), vMIP-II-Eco (5′-CGGAATTCGCGTCCTGGCATA-GACCG-3′), and vMIP-II-Sal (5′-GGGTCGACATTCTTCAGCGAGCAGTG-3′). The amplified vMIP-I and the vMIP-II fragments were digested with *Eco*RI and *Sal*I and inserted downstream of the GST coding of pGEX-5X-1 (GE Healthcare, Uppsala, Sweden) at the *Eco*RI and *Sal*I sites to construct pGEX-vMIP-I and pGEX-vMIP-II. To express a full-length and the deletion mutants of the GST-vMIP-I and GST-vMIP-II fusion protein, the genes for GvM1-Full, GvM1-D1, GvM1-D2,

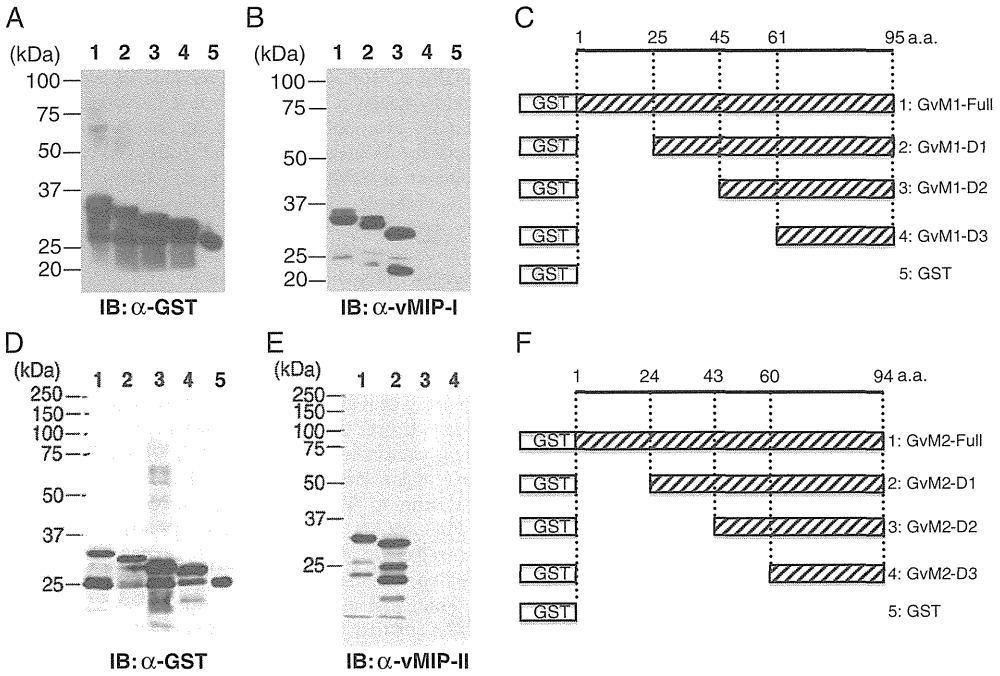

Fig. 2. *Epitope mapping of the anti-vMIP-I and the anti-vMIP-II MAbs. To map the regions of vMIP-I and vMIP-II recognized by the anti-vMIP-I and anti-vMIP-II antibody, a series of* GST-vMIP-I and GST-vMIP-II fusion proteins containing the individual regions of vMIP-I and vMIP-II were constructed as described in Fig. 2C and F, and the proteins were expressed in *E. coli*. The lysates of the fusion proteins, vMIP-I and vMIP-II, and its deletion mutants were immunoblotted with an anti-GST antibody (A and D) and an anti-vMIP-I (B) and an anti-vMIP-II antibody (E) to detect GST-vMIP-I or GST-vMIP-II fusion proteins. Lane 1, GvM1-Full; lane 2, GvM1-D1; lane 3, GvM1-D2; lane 4, GvM1-D3; lane 5, GvM1-D4; lan3 6, GST in Fig. 2A and B. Lane 1, GvM2-Full; lane 2, GvM2-D1; lane 3, GvM2-D2; lane 4, GvM2-D3; lane 5, GST (in D only) in Fig. 2D and E. Summary of GST-vMIP-I (C) and GST-vMIP-II (F) deletion mutants. Individual regions of vMIP-I and vMIP-II were cloned in-frame into the pGEX-5X-1 vector to generate GST-vMIP-I and GST-vMIP-II fusion proteins, respectively. The boxes at left indicate GST, and the white boxes with slashed lines indicate individual domains of vMIP-I and vMIP-II. 1, GvM1-Full(1-95a.a.); 2, GvM1-D1(25-95a.a.); 3, GvM1-D2(45-95a.a.); 4, GvM1-D3(61-95a.a.) in Fig. 2C, and 1, GvM2-Full(1-94a.a.); 2, GvM2-D1(24-94a.a.); 3, GvM2-D2(43-94a.a.); 4, GvM2-D3(60-94a.a.) in Fig. 2F.

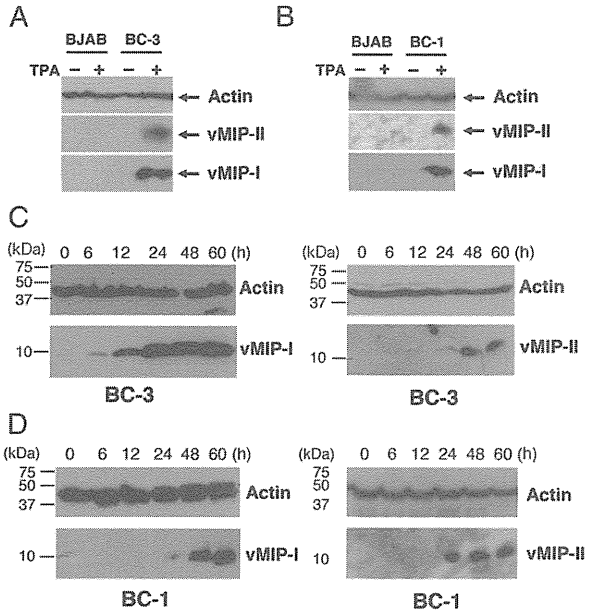

Fig. 3. Detection of vMIP-I and vMIP-II gene products in a KSHV-infected PEL cell line. BC-1 and BC-3 cells were treated with TPA for the indicated number of hours, and the whole-cell extract was prepared after the indicated time post-induction. vMIP-I and vMIP-II were detected by Western blotting and IFA with anti-vMIP-I and -vMIP-II antibodies. Western blot analysis of protein extracted from BC-3 and BJAB cells (A), and BC-1 and BJAB cells (B) with either the anti-vMIP-I or the anti-vMIP-II MAb. Arrows indicate actin, vMIP-I, and vMIP-II proteins. As expected, the estimated sizes of the vMIP-I and vMIP-II proteins, based on comparisons with the migration of molecular size markers, was around 10 kDa. Expression kinetics of vMIP-I (left panel) and vMIP-II (right panel) in TPA-treated BC-3 (C) and BC-1 (D) cells by Western blot analysis. BC-1 and BC-3 cells were harvested after 6, 12, 24, 48, and 60 h post-induction. The lysate was subjected to Western blot analysis as in (A).

GvM1-D3, GvM2-Full, GvM2-D1, GvM2-D2, and GvM2-D3 genes were generated by PCR using the following primer sets: vMIP-I-1F (5′-ATGAATTCCAGATGGCCCCCGTCCAC-3′) and vMIP-I-5R (5′-CCGTGTCGACCGTCTAAGCTATGGCAGGCAGC-3′); vMIP-I-2F (5′-ATGAATTCGCGGGGTCACTCGTGTCG-3′) and vMIP-I-5R; vMIP-I-3F (5′-ATGAATTCCCGCCCGTCCAAATTC-3′) and vMIP-I-5R; vMIP-I-4F (5′-ATGAATTCCCAAAACCCGGAGTTATTTTGC-3′) and vMIP-I-5R; vMIP-II-1F (5′-CGGAATTCGTTATGGACACCAAGGGC-3′) and vMIP-II-5R (5′-GGCAGTCGACTCTTCAGCGAGCAGTGACTG-3′); vMIP-II-2F (5′-GGGAATTCCTGGGAGCGTCCTGGCATAGAC-3′) and vMIP-II-5R; vMIP-II-3F (5′- AAGAATTCTTACCACAGGTGCTTCTGTCC-3′) and vMIP-II-5R; and vMIP-II-4F (5′-TGGAATTCAAGCCGGGTGTGATATTTTTG-3′) and vMIP-II-5R. The PCR products were cloned into pCR2.1 (Invitrogen, Carlsbad, CA) and confirmed by sequencing. The products were digested with the *Eco*RI and *Sal*I restriction enzymes and were cloned into pGEX-5X-1 (GE Healthcare). The PCR conditions for all products were as follows: 25 cycles of 94 °C for 1 min, 55 °C for 1 min, and 72 °C for 2 min in a TP480 PCR thermal cycler (Takara Shuzo, Kyoto, Japan).

Immunization and generation of monoclonal Abs against vMIP-I and vMIP-II

In mice, anti-vMIP-I and -vMIP-II antibodies were raised against the GST-vMIP-I and GST-vMIP-II fusion protein, respectively. These GST fusion proteins were purified on a glutathione-Sepharose 4B column (GE Healthcare), and the GST-vMIP-I and the GST-vMIP-II fusion proteins were conjugated to keyhole limpet hemocyanin KLH (Calbiochem. Co., La Jolla, CA). Mice were initially immunized with 250 μg each of the purified GST-vMIP-I or -II fusion protein in Freund's complete adjuvant administered to the peritoneal cavity, and 200 μg of the antigen in Freund's incomplete adjuvant were injected again 14 and 28 days after the first injection. The mice were exsanguinated 7 days after the last injection. To generate MAbs against vMIP-I and vMIP-II, hybridomas were established by fusing splenocytes from the hyperimmune mice using a nonproducing myeloma cell line, Sp-2/0-Ag14 (ATCC, Manassas, VA). After selection in medium containing hypoxanthine-aminopterin-thymidine, cells secreting MAbs were screened by immunofluorescence assays (IFA). The TPA-induced and -uninduced BCBL-1 cells were fixed in acetone and exposed to supernatants of the hybrid cells. Clones secreting antibodies reactive with TPA-stimulated BCBL-1 cells were expanded and isolated by limiting dilutions.

Transfection analysis of vMIP-I and vMIP-II

To express the vMIP-I and vMIP-II proteins, 293/EBNA cells were transfected with pCAGGS-vMIP-I and -vMIP-II plasmids using TransIT-LT1 (Mirus Bio LLC, Madison, WI). The transfected cells were incubated for 48 h in DMEM supplemented with 10% FCS. The cells were harvested and lysed with lysis buffer (0.05 M Tris-HCl [pH 8.0], 0.15 M NaCl, 0.5% sodium deoxycholate, 1% Triton X-100, 0.1% sodium-dodecyl sulfate [SDS]). The cell lysate was fractionated by electrophoresis on 16% polyacrylamide gel as described below.

Antibodies and Western blotting

The expression of vMIP-I and vMIP-II in BC-3 cells stimulated with TPA was determined with MAbs against vMIP-I and vMIP-II, respectively, as noted above. The concentration of proteins extracted from BC-3 cells was normalized using a BCA Protein Assay Kit (Thermo Fisher Scientific Inc., Rockford, IL). The samples were subjected to SDS-15% polyacrylamide gel electrophoresis under reducing conditions, and were electrophoretically transferred to PVDF membranes (Bio-Rad Laboratories, Hercules, CA). The membranes were blocked for 1 h while being shaken at room temperature in PBS containing 0.05% Tween 20 and 5% w/v nonfat skim milk. The membranes were incubated with a primary antibody and were then incubated for 1 h with an appropriate dilution of horseradish peroxidase (HRP)-conjugated goat anti-mouse IgG antibodies (Santa Cruz Biotechnologies, Santa Cruz, CA). The primary antibody against actin, anti-actin (Ab-1) mouse MAb, was purchased from Merck (Merck KGaA, Darmstadt, Germany). The bound HRP-labeled antibodies were detected with a West Pico substrate kit for horseradish peroxidase (Thermo Fisher Scientific Inc).

IFA

BC-3 cells (10^7 cells) in RPMI 1640 medium with supplements were induced with 25 ng/ml TPA (Sigma Chemical Co., St. Louis, MO). The cells were collected after 0, 4, 8, 12, 24, 48, and 60 h for analysis of the expression kinetics, and for cellular localization analysis 48 h after exposure to TPA. The cells were washed in phosphate-buffered saline (PBS), pH 7.4, and spotted on glass slides. The spots were air-dried, then fixed in ice-cold acetone for 10 min. The cells were then washed with a washing buffer (PBS supplemented with 0.1% Triton X-100) for 15 min, and incubated with either an anti-vMIP-I or an anti-vMIP-II MAb (diluted 1:100 in IFA dilution buffer [PBS containing 2% bovine serum albumin, 0.2% Tween-20, and 0.05% NaN_3]) for 1 h at 37 °C. Then, the slides were washed with the washing buffer, and incubated for 1 h at room temperature with a pre-standardized diluted fluorescein isothiocyanate (FITC)-conjugated goat anti-mouse IgG (Tago Immunologicals, Camarillo, CA). The slides were washed and stained with 4′, 6′-diamidino-2-phenylindole (DAPI) to detect nuclei and were mounted with 50% (v/v) glycerol in PBS. For formalin-fixed paraffin-embedded tissues, antigen retrievals were performed on the de-paraffined sections using citrate buffer. Alexa 488 or 568-conjugated

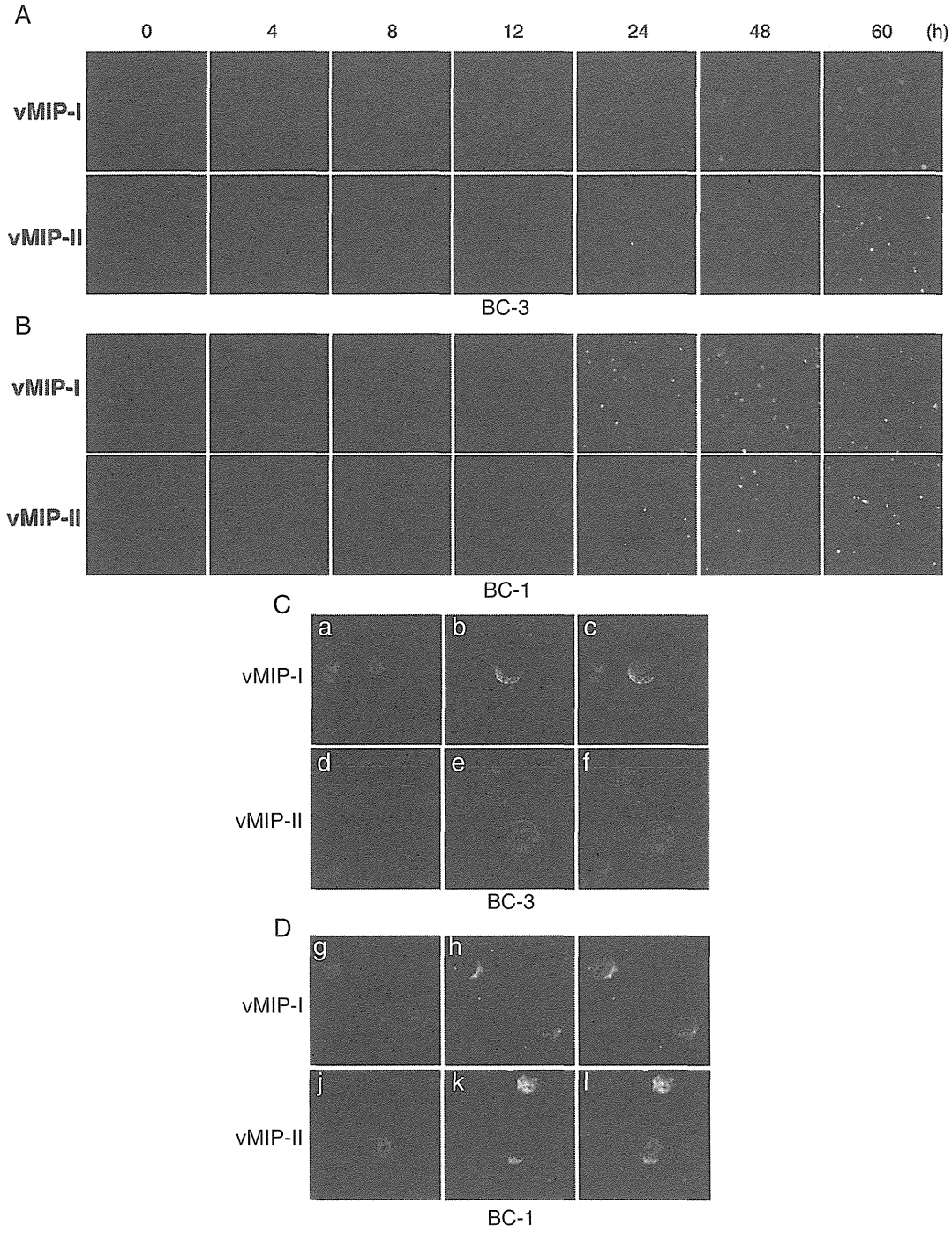

Fig. 4. Expression of vMIP-I and vMIP-II in BC-3 and BC-1 cells by IFA. After 4, 8, 12, 24, 48, and 60 h, BC-3 (A) and BC-1 (B) cells were labeled either with the anti-vMIP-I (upper) or the anti-vMIP-II (lower) MAb followed by goat anti-mouse FITC-conjugated Abs. FITC photomicrographs showing anti-vMIP-I and anti-vMIP-II immunoreactivity in BC-3 and BC-1 cells treated with TPA. (C) Cellular localization of vMIP-I and vMIP-II in BC-3 (C) and BC-1 (D) cells. The cells were stained with DAPI (a, d, g and j), and the localization of vMIP-I and vMIP-II was visualized by IFA with anti-vMIP-I or -vMIP-II MAbs (b, e, h and k); panel a and b, d and e, g and h, and j and k were merged (c, f, i and l). Fluorescence photomicrographs revealed anti-vMIP-I and -vMIP-II immunoreactivity using FITC-conjugated anti-mouse IgG MAb.

anti-mouse or rabbit antibodies (Invitrogen) were used as the secondary antibodies. Confocal microscopic analysis was performed (FV-1000, Olympus, Tokyo, Japan), and the contrast was adjusted before the images were exported as TIFF files to Adobe Photoshop.

Immunohistochemistry

Formalin-fixed paraffin-embedded tissues from KS and MCD patients, and those from an animal model of KSHV-associated solid lymphoma

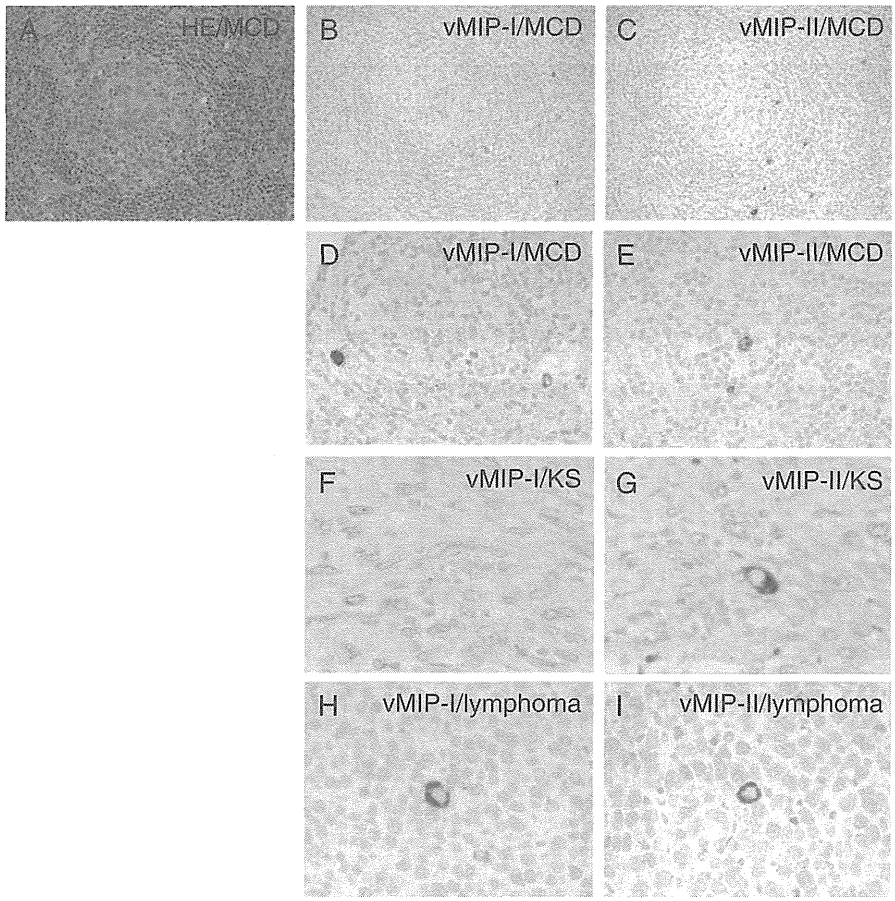

Fig. 5. Expression of vMIP proteins in KSHV-associated diseases. (A–C) Hematoxylin and eosin staining and immunohistochemistry for vMIPs in serial sections of a tissue sample from a patient with MCD. Brown stains indicate positive signals. The nucleus was counter-stained by hematoxylin. (D and E) Higher magnification view of vMIPs expression in an MCD case. Some large lymphocytes in the mantle zone were stained. (F and G) vMIP-I and vMIP-II expression in a KS sample. (H and I) Expression of vMIPs in an animal model of KSHV-associated lymphoma in SCID mice.

were sectioned and stained with hematoxylin and eosin (H&E). Immunohistochemistry of the serial sections was performed with either the anti-vMIP-I or -II MAb. For the second- and third- phase reagents used for immunostaining, a CSAII kit (DAKO, Copenhagen, Denmark) was used. An animal model of KSHV-associated solid lymphoma, which was established as described previously (Katano et al., 2000b), was also subjected to immunohistochemical analysis. Briefly, TY-1 cells were inoculated into the subcutaneous tissue of mice with severe combined immunodeficiency (SCID). One month after inoculation, lymphomas appeared in the subcutaneous region at the inoculation site. Lymphoma cells contained the KSHV genome, and expressed various viral proteins of KSHV (Katano et al., 2000b).

Table 1
Expression of vMIP-I and vMIP-II in MCD and KS tissue samples.

	KSHV proteins, (+)/total	
Cases	vMIP-I	vMIP-II
MCD	(3)/3	(3)/3
KS	(0)/5	(2)/8

Chemotaxis assays

Chemotaxis assays were performed as described previously (Nakano et al., 2003). Briefly, THP-1 cells were washed twice with chemotaxis buffer, 0.5% bovine serum albumin, 20 mM HEPES, pH 7.4, in RPMI 1640. Migration of cells was assessed in a cell culture chamber (Costar, Cambridge, MA), with the upper and lower compartments separated by a 3 μm pore size polycarbonate filter (???). The lower compartment of the chamber was filled with dilutions of vMIP-I, vMIP-II (R&D Systems, Minneapolis, MN) or with PBS alone, and/or with each 10 μg/ml anti-vMIP-I or -vMIP-II MAbs at a volume of 600 μl. The upper compartment contained 100 μl of THP-1 cell suspensions in chemotaxis buffer (10^5 cells/well). The chambers were then incubated for 4 hours at 37 °C, 5% CO_2, and spun at 300 x g, 4 °C, for 5 min. Finally, the cells from the lower compartment were counted.

Results

Specificity of the anti-vMIP-I MAb and the anti-vMIP-II MAb

In order to check specificity of the MAbs, we transfected vMIP-I and vMIP-II expression vectors (pCAGGS-vMIP-I, and -II) into 293/EBNA

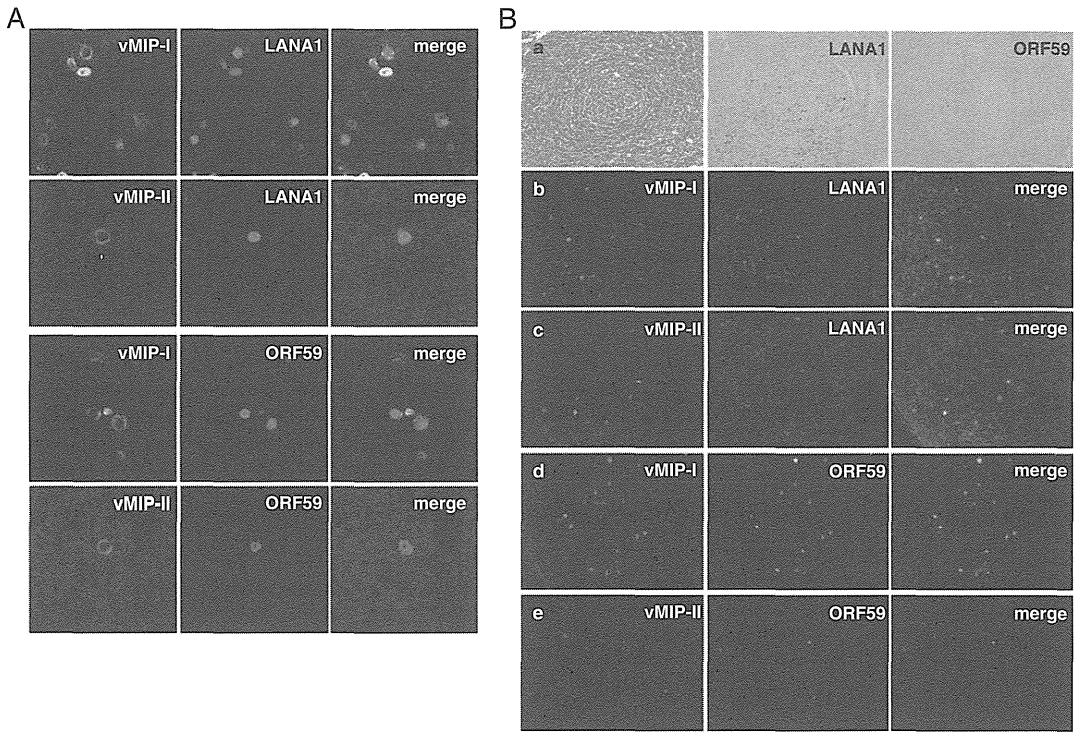

Fig. 6. (A) Expression of vMIPs. LANA1 and ORF59 in the animal model of KSHV-associated solid lymphoma by confocal microscopy. vMIPs were labeled with Alexa 488 (green). LANA1 (upper panels) and ORF59 (lower panels) were labeled with Alexa 568 (red). (B) Expression of vMIPs in MCD. (a) HE staining and immunohistochemistry of LANA1 and ORF59. (b–e) Immunofluorescence assay on MCD lesion. A germinal center is shown in the center of each panel. This case is KSHV-positive large B cell lymphoma arising in MCD.

cells, respectively. The total lysate of the transfected cells was subjected to Western blot analysis. vMIP-I and vMIP-II proteins were detected with anti-vMIP-I or vMIP-II MAbs, respectively (Fig. 1). These antibodies did not show cross-reactivity each other.

Epitope mapping of the anti-vMIP-I and anti-vMIP-II MAbs

We established hybridoma clones secreting MAbs against vMIP-I and vMIP-II, respectively. To map the regions of vMIP-I and vMIP-II where anti-vMIP-I and anti-vMIP-II antibody reacted, a series of GST-fused vMIP-I and vMIP-II deleted proteins were constructed as described in Fig. 2C and F, and used for Western blot analysis with an anti-GST antibody (Santa Cruz Biotechnology Inc), (Fig. 1A, D) and the anti-vMIP-I or the anti-vMIP-II (Fig. 1B, E) antibody, respectively. The results showed that all GST-vMIP-I and GST-vMIP-II fusion proteins interacted with the anti-GST antibody (Fig. 2A, D) and showed that GvM1-Full, GvM1-D1, and GvM1-D2 reacted with the anti-vMIP-I antibody, whereas GvM1-D3 did not (Fig. 1B), and GvM2-Full and GvM2-D1 reacted with the anti-vMIP-II antibody, whereas GvM2-D2, and GvM2-D3 did not (Fig. 2E). Thus, these results demonstrated that an anti-vMIP-I MAbs was successfully generated and suggest that the amino acid residues 61 to 95 of vMIP-I could be a major epitope reacted with the anti-vMIP-I antibody. On the other hand, the amino acid residues 24 to 42 of vMIP-II could be an epitope reacted with the anti-vMIP-II antibody.

Expression of vMIP-I and vMIP-II in the KSHV-infected PEL cell line

We tested vMIP-I and vMIP-II expression in KSHV and Epstein Barr virus (EBV) dually infected PEL cell lines (BC-1), KSHV infected PEL cell lines (BC-3) and in non-infected Burkitt's lymphoma cell line (BJAB), and detected them in TPA-stimulated BC-3 and BC-1 cells with developed antibodies, but not in BJAB cells non-stimulated BC-3 or BC-1 cells (Fig. 2A, B). In a KSHV infected PEL cells, BC-1 and BC-3, vMIP-I and vMIP-II were detected around at 10 kDa, which matches the size deduced from amino acids length (Fig. 3C, D). Actually, vMIP-I was detected from 6 hours post induction and vMIP-II was at 24 hours in BC-3 cells (Fig. 3C), and vMIP-I and vMIP-II were detected at 24 h in BC-1 cells (Fig. 3D). In the immunofluorescence microscopy, the number of vMIP-II expressing cells seemed to be more than that of vMIP-I in BC-3 cells (Fig. 4A, B). In order to analyze the cellular localization of vMIP-I and vMIP-II protein, BC-3 and BC-1 cells stimulated with TPA were doubly labeled with DAPI (Fig. 4C, a, d and D, g, j), and either the anti-vMIP-I MAb (Fig. 4C, b and D, h) or the anti-vMIP-II MAb (Fig. 4C, e and D, k). Merged images were shown in Fig. 4C, c, f, and D, i, l). The vMIP-I and the vMIP-II clearly showed cytoplasm and possibly membranes in TPA-induced BC-3 and BC-1 cells (Fig. 4C, b, e, and D, h, k).

Expression of vMIPs in KSHV-associated diseases

To know the expression of vMIPs in KSHV-associated diseases, immunohistochemistry for vMIPs was performed on pathological samples of eight KS cases, three MCD cases, and the animal model of KSHV-associated solid lymphoma (Fig. 5). Immunohistochemistry demonstrated that vMIP-I and vMIP-II were detected in some cells in the mantle zone of germinal center and the interfollicular zone in KSHV-positive MCD samples (Fig. 5A to E). Both vMIP-I and vMIP-II were detected predominantly in the cytoplasm of large lymphocytes. The numbers of positive cells varied among three MCD cases examined. On the other

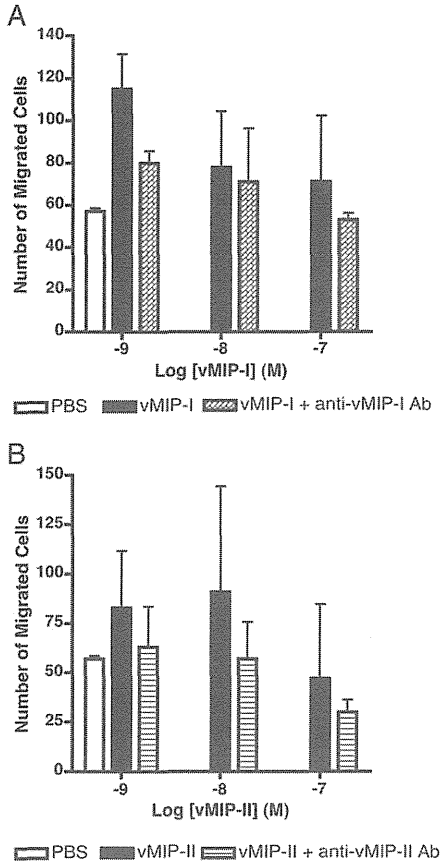

Fig. 7. Neutralizing activity of anti-vMIP-I and -vMIP-II MAbs. THP-1 cell migration in response to increased concentrations of vMIP-I and vMIP-II (1, 10, 100 nM), and the neutralizing activity of 10 μg/ml anti-vMIP-I and -vMIP-II MAbs against vMIP-I and vMIP-II were measured, as outlined in Materials and Methods, by using the transwell migration assay system. Various doses of vMIP-I and vMIP-II were tested for their ability to induce the chemotaxis of THP-1 cells. The data presented are from one experiment, and are representative of the triplicate experiments performed. The error bars indicate the standard deviations of three independent experiments.

hand, any positive signal of vMIP-I was not observed in all KS cases (Fig. 5F, G). vMIP-II was rarely detected in the cytoplasm of spindle cells in two KS cases at the nodular stage out of eight KS cases. In the samples of animal model of KSHV-associated solid lymphoma, both vMIP-I and vMIP-II were detected in the cytoplasm of a part of lymphoma cells (Fig. 5H, I). These data showed that vMIP-I and vMIP-II were expressed in cells in MCD and KSHV-associated lymphoma, but vMIP-II was rarely in KS (Table 1). To know the association of vMIPs expression with expression of other KSHV-encoded proteins, we examined immunofluorescence assay on KSHV-associated diseases. Since, all KSHV-infected cells express LANA1, vMIPs-positive cells were positive for LANA1. However, expression pattern of LANA1 showed diffuse nuclear staining in vMIPs-positive cells in the animal model of KSHV-associated solid lymphoma (Fig. 6A). Confocal microscopy revealed that vMIP-I stain showed usually cytoplasmic pattern, but rarely diffuse nuclear staining pattern *in vivo*. Almost all cells with vMIPs expression were also positive for ORF59 protein, a lytic protein of KSHV. IFA also demonstrated that vMIPs-positive cells expressed LANA1 at various levels in MCD clinical samples (Fig. 6B, a to c). A large portion of vMIPs-positive cells also expressed ORF59 protein in MCD (Fig. 6B, d, e). These data suggest that vMIPs are expressed by cells with KSHV-lytic infection in KSHV-associated MCD and lymphoma.

Neutralization of vMIP-I and vMIP-II by anti-vMIP-I and anti-vMIP-II MAbs

We examined whether the anti-vMIP-I and anti-vMIP-II MAbs could neutralize the chemoattractant of vMIP-I and vMIP-II to induce the migration of THP-1 cells. As expected, vMIP-I and vMIP-II induced migration of THP-1 cells (Fig. 7A, B), but not with PBS alone. However, anti-vMIP-I and anti-vMIP-II MAbs inhibited respective vMIP-I and vMIP-II-induced cell migration of THP-1 cells at 10 μg/ml final concentration.

Discussions

It was known that KSHV encodes three chemokine genes of the so-called viral macrophage inflammatory proteins: *vMIP-I*, *vMIP-II*, and *vMIP-III* in the genome. Analysis of the translated amino acid sequence indicate that the vMIP-I and vMIP-II gene have four conserved cysteines capable of forming two essential disulfide bonds (first cysteine and third cysteine, and second cysteine and fourth cysteine). The family of chemokines comprises CC, CXC, C, and CX_3C subfamilies. The vMIP-I and vMIP-II have four cysteines, the first two of which are found in the sequence of CC, which correspond to the CC profile. These gene products were expressed in the phase of KSHV lytic infection (Moore et al., 1996; Sun et al., 1999). Both vMIP-I and vMIP-II were expressed in a KSHV-infected cell lines, BC-3, which had been treated with TPA. Mono-specific polyclonal Abs against vMIP-I and vMIP-II have been described in previous studies that investigated the localization of vMIPs in PEL cells (Nakano et al., 2003). In the present study, we developed the respective MAbs that reacted either with KSHV vMIP-I or vMIP-II. We first applied these MAbs against KSHV vMIP-I and vMIP-II to detect KSHV-infected BC-3 and BC-1 cells by Western blotting and immunofluorescence assay. The Western blot analysis revealed that both the anti-vMIP-I and the anti-vMIP-II MAbs reacted to the 10-kDa proteins considered specific to the respective vMIP protein. The anti-vMIP-I MAb was shown to be reactive with the epitopes in the middle of the protein (sequence, PPVQILKEWYPTSPAC), and the epitope of the anti-vMIP-II MAb was shown to be reactive at the N-terminal end (sequence, LGASWHRPDKCCLGYQKRP). Further immunofluorescence analysis of the cellular localization of both vMIP-I and vMIP-II with anti-vMIP-I and anti-vMIP-II MAb showed a cytoplasmic pattern of expression in BC-3 and BC-1 cells. As the results indicated that these gene products were expressed in the cytoplasm, it might be located at the KSHV-infected BC-3 or BC-1 cells membrane prior to secretion. An investigation of the antigenic specificities of MAbs against KSHV vMIP-I and vMIP-II in MCD and KS patients has not yet been reported. Here, immunohistochemical analysis detected only vMIP-II in samples from both KS and MCD patients, but vMIP-I was not detected in KS cases: however, both vMIP-I and vMIP-II proteins were expressed in some cells in the interfollicular zone of MCD tissues. Lytic proteins of the KSHV such as K8, RTA, and ORF59 have been detected in large lymphocytes in the mantle zone of MCD cases (Dupin et al., 1999; Katano et al., 2000a). The expression of vMIPs showed a similar pattern to that of the lytic proteins in MCD tissues. In contrast, lytic protein expression, including that of vMIPs, was rare in the KS lesions (Abe et al., 2006). In the present study, we demonstrated that vMIPs were expressed in the cells expressing ORF59 protein. Thus, our data clearly indicated that the expression of vMIPs is associated with lytic infection in individual cells affected by KSHV-associated diseases. Human monocytic cell line THP-1 respond to various chemokines suggesting that they express receptors for these chemokines (Wang et al., 1993). Previous study, vMIP-I and vMIP-II were shown chemotaxis in THP-1 cells (Nakano et al., 2003). It has been reported that vMIP-I acts as a specific agonist for CC chemokine receptor 8 (CCR8) (Dairaghi et al., 1999; Endres et al., 1999) and vMIP-II shows a Ca^{2+} flux as a specific agonist for CCR3 (Boshoff et al., 1997). Our data showed anti-vMIP-I and anti-vMIP-II MAbs were able to neutralize vMIP-I- and vMIP-II-mediated chemotaxis in THP-1 cells. However, neutralizing activities

of anti-vMIP-I MAb was apparently low, even the addition of 10 μg/ml MAbs. These findings support the assumption that anti-vMIP-I and –vMIP-II MAbs-blocked chemotaxis in THP-1 cells act through binding to the certain amino acid residue of vMIP-I and vMIP-II.

In summary, MAbs developed specifically for this series were used to detect vMIP-I and vMIP-II in MCD and KS tissues, which may account for certain clinical features of MCD and KS. To gain a better understanding of these important viral genes, additional studies will be needed that focus on revealing vMIP-I and vMIP-II expression profiles during lytic infection. Taken together, these studies provide an insight into the pathogenesis of the contribution of vMIP-I and vMIP-II to the lytic induction of KSHV. These MAbs could serve as useful tools to clarify the pathogenesis of KSHV-related diseases.

Acknowledgments

This study was supported by a grant for Research on Publicly Essential Drugs and Medical Devices from the Japan Health Sciences Foundation (SAA4832), Health and Labor Sciences Research Grants (to HK, No. H23-AIDS-Ippan-002) from the Ministry of Health and by a grant from PRESTO of the Japan Science and Technology Corporation (200154023).

References

Abe, Y., Matsubara, D., Gatanaga, H., Oka, S., Kimura, S., Sasao, Y., Saitoh, K., Fujii, T., Sato, Y., Sata, T., Katano, H., 2006. Distinct expression of Kaposi's sarcoma-associated herpesvirus-encoded proteins in Kaposi's sarcoma and multicentric Castleman's disease. Pathol. Int. 56, 617–624.

Arvanitakis, L., Mesri, E.A., Nador, R.G., Said, J.W., Asch, A.S., Knowles, D.M., Cesarman, E., 1996. Establishment and characterization of a primary effusion (body cavity-based) lymphoma cell line (BC-3) harboring kaposi's sarcoma-associated herpesvirus (KSHV/HHV-8) in the absence of Epstein-Barr virus. Blood 88, 2648–2654.

Benelli, R., Barbero, A., Buffa, A., Aluigi, M.G., Masiello, L., Morbidelli, L., Ziche, M., Albini, A., Noonan, D., 2000. Distinct chemotactic and angiogenic activities of peptides derived from Kaposi's sarcoma virus encoded chemokines. Int. J. Oncol. 17, 75–81.

Boshoff, C., Endo, Y., Collins, P.D., Takeuchi, Y., Reeves, J.D., Schweickart, V.L., Siani, M.A., Sasaki, T., Williams, T.J., Gray, P.W., Moore, P.S., Chang, Y., Weiss, R.A., 1997. Angiogenic and HIV-inhibitory functions of KSHV-encoded chemokines. Science 278, 290–294.

Cesarman, E., Chang, Y., Moore, P.S., Said, J.W., Knowles, D.M., 1995. Kaposi's sarcoma-associated herpesvirus-like DNA sequences in AIDS-related body-cavity-based lymphomas. N. Engl. J. Med. 332, 1186–1191.

Chang, Y., Cesarman, E., Pessin, M.S., Lee, F., Culpepper, J., Knowles, D.M., Moore, P.S., 1994. Identification of herpesvirus-like DNA sequences in AIDS-associated Kaposi's sarcoma. Science 266, 1865–1869.

Chen, S., Bacon, K.B., Li, L., Garcia, G.E., Xia, Y., Lo, D., Thompson, D.A., Siani, M.A., Yamamoto, T., Harrison, J.K., Feng, L., 1998. In vivo inhibition of CC and CX3C chemokine-induced leukocyte infiltration and attenuation of glomerulonephritis in Wistar–Kyoto (WKY) rats by vMIP-II. J. Exp. Med. 188, 193–198.

Dairaghi, D.J., Fan, R.A., McMaster, B.E., Hanley, M.R., Schall, T.J., 1999. HHV8-encoded vMIP-I selectively engages chemokine receptor CCR8. Agonist and antagonist profiles of viral chemokines. Biol. Chem. 274, 21569–21574.

Dupin, N., Fisher, C., Kellam, P., Ariad, S., Tulliez, M., Franck, N., van Marck, E., Salmon, D., Gorin, I., Escande, J.P., Weiss, R.A., Alitalo, K., Boshoff, C., 1999. Distribution of human herpesvirus-8 latently infected cells in Kaposi's sarcoma, multicentric Castleman's disease, and primary effusion lymphoma. Proc. Natl. Acad. Sci. U. S. A. 96, 4546–4551.

Endres, M.J., Garlisi, C.G., Xiao, H., Shan, L., Hedrick, J.A., 1999. The Kaposi's sarcoma-related herpesvirus (KSHV)-encoded chemokine vMIP-I is a specific agonist for the CC chemokine receptor (CCR)8. J. Exp. Med. 189, 1993–1998.

Katano, H., Sato, Y., Kurata, T., Mori, S., Sata, T., 2000a. Expression and localization of human herpesvirus 8-encoded proteins in primary effusion lymphoma, Kaposi's sarcoma, and multicentric Castleman's disease. Virology 269, 335–344.

Katano, H., Suda, T., Morishita, Y., Yamamoto, K., Hoshino, Y., Nakamura, K., Tachikawa, N., Sata, T., Hamaguchi, H., Iwamoto, A., Mori, S., 2000b. Human herpesvirus 8-associated solid lymphomas that occur in AIDS patients take anaplastic large cell morphology. Mod. Pathol. 13, 77–85.

Kledal, T.N., Rosenkilde, M.M., Coulin, F., Simmons, G., Johnsen, A.H., Alouani, S., Power, C.A., Luttichau, H.R., Gerstoft, J., Clapham, P.R., Clark-Lewis, I., Wells, T.N., Schwartz, T.W., 1997. A broad-spectrum chemokine antagonist encoded by Kaposi's sarcoma-associated herpesvirus. Science 277, 1656–1659.

Miller, G., Heston, L., Grogan, E., Gradoville, L., Rigsby, M., Sun, R., Shedd, D., Kushnaryov, V.M., Grossberg, S., Chang, Y., 1997. Selective switch between latency and lytic replication of Kaposi's sarcoma herpesvirus and Epstein-Barr virus in dually infected body cavity lymphoma cells. J. Virol. 71, 314–324.

Moore, P.S., Boshoff, C., Weiss, R.A., Chang, Y., 1996. Molecular mimicry of human cytokine and cytokine response pathway genes by KSHV. Science 274, 1739–1744.

Nakano, K., Isegawa, Y., Zou, P., Tadagaki, K., Inagi, R., Yamanishi, K., 2003. Kaposi's sarcoma-associated herpesvirus (KSHV)-encoded vMIP-I and vMIP-II induce signal transduction and chemotaxis in monocytic cells. Arch. Virol. 148, 871–890.

Niwa, H., Yamamura, K., Miyazaki, J., 1991. Efficient selection for high-expression transfectants with a novel eukaryotic vector. Gene 108, 193–199.

Schalling, M., Ekman, M., Kaaya, E.E., Linde, A., Biberfeld, P., 1995. A role for a new herpes virus (KSHV) in different forms of Kaposi's sarcoma. Nat. Med. 1, 707–708.

Soulier, J., Grollet, L., Oksenhendler, E., Cacoub, P., Cazals-Hatem, D., Babinet, P., d'Agay, M.F., Clauvel, J.P., Raphael, M., Degos, L., et al., 1995. Kaposi's sarcoma-associated herpesvirus-like DNA sequences in multicentric Castleman's disease. Blood 86, 1276–1280.

Sun, R., Lin, S.F., Staskus, K., Gradoville, L., Grogan, E., Haase, A., Miller, G., 1999. Kinetics of Kaposi's sarcoma-associated herpesvirus gene expression. J. Virol. 73, 2232–2242.

Wang, J.M., McVicar, D.W., Oppenheim, J.J., Kelvin, D.J., 1993. Identification of RANTES receptor on human monocytic cells: competition of binding and desensitization by homologous chemotactic cytokines. J. Exp. Med. 177, 699–705.

OPEN ACCESS Freely available online

PLOS ONE

Predictive Clinical Factors in the Diagnosis of Gastrointestinal Kaposi's Sarcoma and Its Endoscopic Severity

Naoyoshi Nagata[1]*, Takuro Shimbo[2], Hirohisa Yazaki[3], Naoki Asayama[1], Junichi Akiyama[1], Katsuji Teruya[3], Toru Igari[4], Norio Ohmagari[5], Shinichi Oka[3], Naomi Uemura[6]

1 Department of Gastroenterology and Hepatology, National Center for Global Health and Medicine, Tokyo, Japan, **2** Clinical Research and Informatics, International Clinical Research Center Research Institute, National Center for Global Health and Medicine, Tokyo, Japan, **3** Division of AIDS Clinical Center, National Center for Global Health and Medicine, Tokyo, Japan, **4** Department of Clinical Pathology, National Center for Global Health and Medicine, Tokyo, Japan, **5** Department of Infectious Disease, National Center for Global Health and Medicine, Tokyo, Japan, **6** Department of Gastroenterology and Hepatology, National Center for Global Health and Medicine, Kohnodai Hospital, Chiba, Japan

Abstract

Background: The diagnosis of gastrointestinal (GI) involvement in Kaposi's sarcoma (KS) is important to make because the need for treatment depends on the extent of the disease. Moreover, severe GI lesions can cause serious complications. Endoscopy with biopsy is an extremely useful method to diagnose GI-KS. However, determining the indications for endoscopy is difficult because KS can occur without GI symptoms or cutaneous KS. This study sought to clarify predictive clinical factors for GI-KS and its severity on endoscopy.

Methodology/Principal Findings: A total of 1,027 HIV-infected patients who underwent endoscopy were analyzed. Sexual behavior, CD4 count, HIV RNA, history of highly active antiretroviral therapy (HAART), GI symptoms, and cutaneous KS were assessed. Endoscopic severity including bulky tumor, ulceration, and number of lesions were evaluated. Thirty-three patients had GI-KS and 46 patients cutaneous KS. Among the GI-KS patients, 78.8% (26/33) had no GI symptoms and 24.2% (8/33) had no cutaneous KS. Univariate analysis identified men who have sex with men (MSM), CD4 $<$100 cells/μL, HIV RNA $\geq$10,000 copies/mL, no history of HAART, and cutaneous KS were significantly associated with GI-KS. Among these factors, cutaneous KS was closely related to GI-KS on multivariable analysis. Among patients without cutaneous KS, MSM and CD4 count $<$100 cells/μL were the only independent clinical factors related to GI-KS. Bulky tumor was significantly associated with CD4 $<$100 cells/μL and large number of lesions was significantly associated with HIV-RNA $\geq$10,000 copies/mL.

Conclusions: To diagnose GI-KS, clinical factors need to be considered before endoscopy. The presence of GI symptoms is not useful in predicting GI-KS. MSM and CD4 count $<$100 cells/μL are predictive factors among patients without cutaneous KS. Caution should be exercised especially in patients with low CD4 counts or high HIV viral loads as they are more likely to develop severe GI-KS lesions.

Citation: Nagata N, Shimbo T, Yazaki H, Asayama N, Akiyama J, et al. (2012) Predictive Clinical Factors in the Diagnosis of Gastrointestinal Kaposi's Sarcoma and Its Endoscopic Severity. PLoS ONE 7(11): e46967. doi:10.1371/journal.pone.0046967

Editor: Jianming Tang, University of Alabama at Birmingham, United States of America

Received June 16, 2012; **Accepted** September 7, 2012; **Published** November 30, 2012

Funding: This study was partly supported by Medicine for Ministry of Health, Labour and Welfare, Health and Labour Sciences Research Grants, Research on Clinical Trials' Infrastructure Development and grants for research and development in National Center for Global Health and Medicine. The funders had no role in study design, data collection and analysis, decision to publish, or preparation of the manuscript.

Competing Interests: The authors have declared that no competing interests exist.

* E-mail: nnagata_ncgm@yahoo.co.jp

Introduction

Kaposi's sarcoma (KS) is a rare type of cancer of the lymphatic and blood vessels that most commonly involves the skin [1–3]. KS is more prevalent in HIV-infected patients, especially among men who have sex with men (MSM) [2,3]. Although the rate of AIDS-related KS has decreased dramatically since the introduction of highly active antiretroviral therapy (HAART) [4–6], KS remains the most common malignancy among patients with AIDS [7].

The diagnosis of visceral involvement of KS is important to make because the need for treatment and choice of treatment depend on the extent of the disease [4–11]. The gastrointestinal (GI) tract is a common site of visceral involvement [12–16]. Endoscopy with biopsy is extremely useful for diagnosing GI-KS and is usually indicated for patients with GI symptoms and the presence of cutaneous KS [17,18]. However, GI-KS can occur without GI symptoms [19,20] and in the absence of cutaneous disease [20,21]. Moreover, few studies have investigated the clinical factors of GI-KS [19–21] and most of those have been case series or case reports without control subjects. Therefore, the indications for endoscopy to detect GI-KS in patients with HIV/AIDS, especially those without GI symptoms or cutaneous disease, have been difficult to determine.

Endoscopically, GI-KS can vary from flat maculopapular or polypoid masses to severe lesions. The latter can cause serious complications such as hemorrhage, perforation, and obstruction

and may require emergent treatment [14,22–26]. However, there are no reports to date on the predictive clinical factors for finding severe GI-KS lesions on endoscopy.

In Japan, screening endoscopy is frequently performed for the early detection of malignant or premalignant lesions, even as part of the examination for patients who are asymptomatic. In this study, we performed endoscopy in a large number of HIV-infected patients with or without GI symptoms and cutaneous involvement.

Methods

Objectives

We conducted a case-control study to identify predictive clinical factors for diagnosing GI-KS, especially among patients without GI symptoms and cutaneous disease. We also assessed macroscopic appearance in detail looking for predictors of severe GI-KS lesions on endoscopy.

Participants

We recruited 1,064 HIV-infected patients who had undergone endoscopy between 2003 and 2009 at the National Center for Global Health and Medicine (NCGM), a 900-bed hospital located in the Tokyo metropolitan area and the largest referral center for HIV/AIDS in Japan. We excluded patients who had received endoscopy for follow-up evaluation shortly after treatment for GI disease.

Ethics statement

The institutional review board at NCGM approved this study. All patients from whom clinical samples were obtained during endoscopy or biopsy had provided written informed consent prior to endoscopy. No ethical problems exist with regard to the publication of this manuscript. We used anonymized data from patient medical records.

Clinical factors

Before endoscopy, we routinely enter "purposes of the inspection" into the electronic endoscopic database. Purposes include examination for symptoms, screening for malignant or premalignant lesions, and follow up for endoscopic procedure or surgery. GI symptoms were assessed by the physician who interviewed each patient in detail. Those without GI symptoms and negative screening endoscopy were considered to be symptom-free.

CD4 cell counts were checked within 1 week of endoscopy. We categorized CD4 cell counts into four groups: $\geq$300 cells/μL; 200–299 cells/μL; 100–199 cells/μL; and $<$100 cells/μL. HIV-RNA viral load (VL) as determined by real-time quantitative polymerase chain reaction (PCR) was reviewed within 1 month of endoscopy. The minimum detection level was 40 copies/mL of plasma. A positive result for real-time HIV RNA was defined as $\geq$40 copies/mL. HIV-RNA VL was categorized into four groups: VL $\leq$40 copies/mL (normal range); 40$<$VL$\leq$10,000 copies/ml; 10,000$<$VL$\leq$100,000 copies/mL; and VL$>$100,000 copies/mL.

History of HAART was collected from medical records prior to endoscopy and was categorized into five groups according to duration of administration: without history of HAART; duration $\leq$6 months; 6 months$<$duration $\leq$1 year; 1 year$<$duration $\leq$5 years; duration $>$5 years.

HIV infection route was determined by the medical staff who interviewed each patient on the first visit to our hospital and classified into five categories: MSM, heterosexual, hemophiliac, injection drug user, and unknown. We defined sexual behavior as MSM or heterosexual. Patients who were not homosexual or bisexual were regarded as heterosexual.

Diagnosis of GI-KS

We performed biopsy when abnormal findings were encountered on upper or lower endoscopy. If we performed both upper and lower endoscopy in the same individual, this was defined as one case. GI-KS was suspected based on endoscopic appearance, such as the presence of submucosal nodules, polypoid nodules, or deep-red mucosa (Fig. 1A–C), as previously reported [16,19,27]. Endoscopic severity was evaluated in terms of appearance, including size, ulceration, and number of lesions. Regarding size, we defined bulky tumors (Fig. 1D) as circumferential or obstructive lesions and small tumors as all other cases [23]. Ulceration was defined endoscopically as a distinct, visible crater $>$5 mm in diameter with a slough base (Fig. 1E). The number of lesions was classified into two groups: large number ($\geq$10) (Fig. 1F) or small number ($<$10).

GI-KS was defined as the presence of proliferating spindle cells in biopsy specimens as seen on hematoxylin and eosin (HE) staining (Fig. 2A). Spindle cells were consistently positive on immunohistochemical staining for D2–40 (Fig. 2B), CD34 (Fig. 2C), and HHV-8 (Fig. 2D), as previously reported [28,29]. We assessed the presence of lesions in the esophagus, stomach, duodenum, terminal ileum, colon, and rectum. Before endoscopy, we examined all patients for cutaneous lesions of KS.

Statistical analysis

After summarizing the descriptive patient characteristics, to identify predictive clinical factors for diagnosing GI-KS, we calculated odds ratios (ORs) and 95% confidence intervals (CIs). The relationship between GI-KS and categories of CD4 cell count, HIV-RNA VL, and HAART duration were evaluated using the chi-square test for linear trends. For multivariable analysis, we used a multiple logistic regression model that included all factors showing values of $p<0.1$ on univariate analysis. Exact logistic regression was also used if the number in a cell was 0. A final model was then developed by backward selection of factors showing values of $p<0.10$.

The relationships between endoscopic severity of GI-KS and clinical factors were also evaluated using the chi-square test. Values of $p<0.10$ were considered significant. All statistical analysis was performed using Stata version 10 software (StataCorp LP, College Station, TX).

Results

Participants

Of the 1,064 potential study subjects recruited who underwent endoscopy, we excluded 37 who underwent endoscopy for follow-up evaluation shortly after treatment for GI diseases. Ultimately, the remaining 1,027 patients were selected for data analysis.

Baseline characteristics

Characteristics of the 1,027 patients with HIV are shown in Table 1. Median age was 44 years (interquartile range [IQR], 36–56 years). Patients were predominantly male (91.8%).

Routes of HIV infection included MSM (67.0%), heterosexual (17.0%), hemophilia (13.6%), drug usage (0.2%), and unknown (2.1%). Median CD4 count was 239 cells/μL (IQR, 100–406 cells/μL). Median HIV-RNA VL was $<$40 copies/mL (IQR, $<$40–33,000 copies/mL). A total of 739 patients (72.0%) had received HAART.

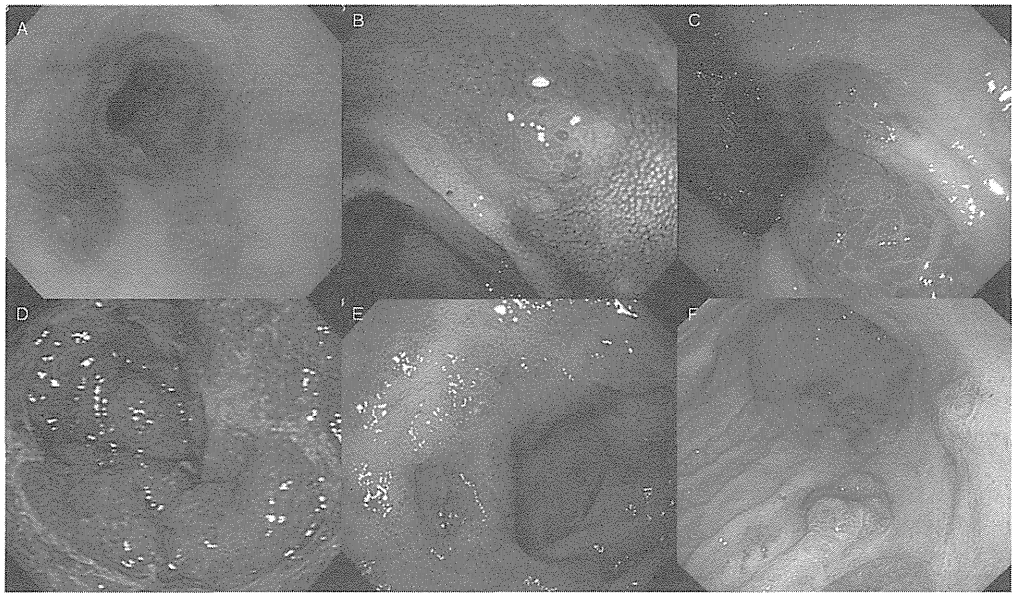

Figure 1. Gastrointestinal Kaposi's sarcoma on endoscopy. A) Dark-reddish flat lesions in the esophagus. **B**) Chromoendoscopy with indigo carmine dye showed a polypoid nodule in the terminal ileum. **C**). Submucosal lesions in the rectum. **D**) Bulky tumor surrounding the antrum of the stomach and causing pyloric stenosis. **E**) Circumferential flat lesions with ulceration in the duodenum. **F**) Multiple nodules in the stomach.
doi:10.1371/journal.pone.0046967.g001

GI symptoms were noted in 368 patients (35.8%) as follows: appetite loss (n = 6); throat pain (n = 8); dysphagia (n = 11); reflux or heartburn (n = 22); epigastric pain (n = 87); nausea or vomiting (n = 36); hematemesis (n = 25); tarry stool (n = 43); hematochezia (n = 54); diarrhea (n = 87); distended abdomen (n = 2); and lower abdominal pain (n = 17).

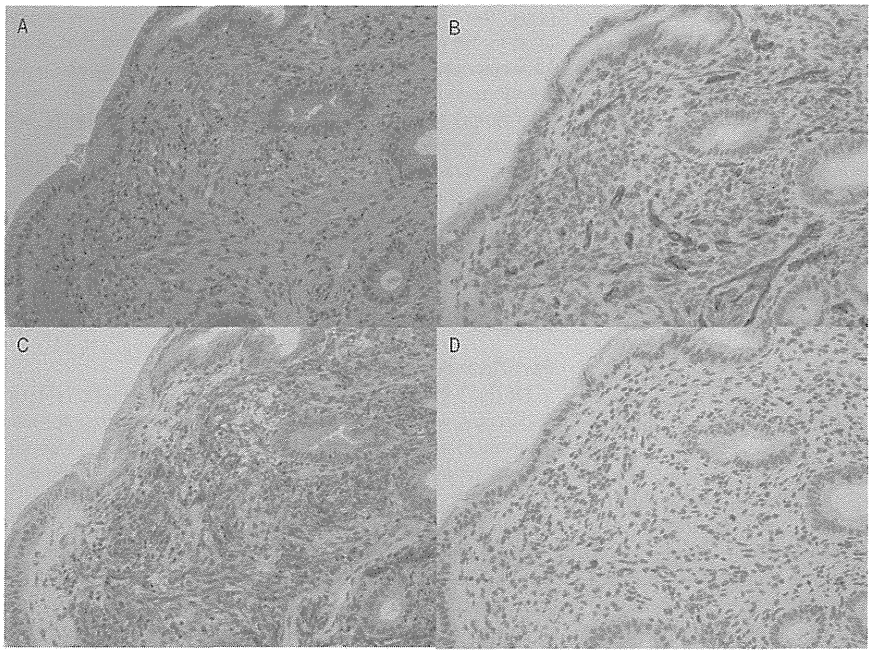

Figure 2. Pathological features of GI-KS. A) Spindle cell proliferation found in the submucosa on hematoxylin and eosin (HE) staining. **B**) Immunohistochemical staining revealing strong expression of CD34. **C**) Immunohistochemical staining revealing expression of D2–40. Vascular gaps are lined with endothelial cells on staining for CD34 and D2–40. **D**) Some endothelial cells are positive for human herpes virus 8 (HHV-8).
doi:10.1371/journal.pone.0046967.g002

Table 1. Patient characteristics.

	All (n = 1,027)	With GI-KS (n = 33)	Without GI-KS (n = 994)
Age, median (IQR)*	44 (36, 56)	44 (36, 56)	45 (35, 55)
Sex (male), n (%)	943 (91.8%)	33 (100%)	910 (91.6%)
HIV infection route, n (%)			
MSM	688 (67.0%)	31 (93.9%)	657 (66.1%)
Heterosexual	175 (17.0%)	2 (6.1%)	173 (17.4%)
Hemophiliac	140 (13.6%)	0	140 (14.1%)
Drug-user	2 (0.2%)	0	2 (0.2%)
Unknown	22 (2.2%)	0	22 (2.2%)
CD4 cell count (cells/μL)			
≥300	424 (41.3%)	1 (3.0%)	423 (42.6%)
200–299	155 (15.1%)	3 (9.1%)	152 (15.3%)
100–199	193 (18.8%)	8 (24.2%)	185 (18.6%)
<100	255 (24.8%)	21 (63.7%)	234 (23.5%)
HIV RNA (copies/mL)			
VL≤40 (normal range)	533 (51.9%)	4 (12.1%)	529 (53.2%)
40<VL≤10,000	176 (17.1%)	4 (12.1%)	172 (17.3%)
10,000<VL≤100,000	151 (14.7%)	7 (21.1%)	144 (14.5%)
VL>100,000	167 (16.3%)	18 (54.6%)	149 (15.0%)
History of HAART, n (%)			
Without history of HAART	288 (28.0%)	18 (54.6%)	270 (27.2%)
Duration ≤6 months	113 (11.0%)	8 (24.2%)	105 (10.6%)
6 months<duration≤1 yr	75 (7.3%)	7 (21.2%)	68 (6.8%)
1 yr<duration≤5 yrs	67 (6.5%)	0	67 (6.7%)
Duration >5 yrs	484 (47.1%)	0	484 (48.7%)
GI symptoms, n (%)			
Without	659 (64.2%)	26 (78.8%)	633 (63.7%)
With	368 (35.8%)	7 (21.2%)	361 (36.3%)
Cutaneous KS			
Without	981 (95.5%)	8 (24.2%)	973 (97.9%)
With	46 (4.5%)	25 (75.8%)	21 (2.1%)

Abbreviations: IQR, interquartile range; MSM, men who have sex with men; VL, viral load; yrs, years; GI, gastrointestinal.
doi:10.1371/journal.pone.0046967.t001

Characteristics of GI-KS

Of the 1,027 patients, 33 (3.2%) were diagnosed with GI-KS (Table 1). GI lesions were found in the esophagus (n = 10), stomach (n = 20), duodenum (n = 17), terminal ileum (n = 7), colon (n = 13), and rectum (n = 9). Of the patients with GI-KS, 78.8% (26/33) had no GI symptoms and 24.2% (8/33) had no cutaneous KS (Table 1).

Five of eight GI-KS patients without cutaneous involvement underwent HAART for a mean duration of 1.84 months.

Predictive clinical factors of GI-KS

Univariate analysis identified MSM, CD4 count <100 cells/μL, HIV RNA VL ≥10,000 copies/mL, no history of HAART, and the presence of cutaneous KS as significant clinical factors for the development of GI-KS (Table 2).

As the CD4 count decreased (≥300; 200–299; 100–199; and <100 cells/μL), occurrence of GI-KS increased significantly ($p<0.01$ for trend in odds, Table 1). As HIV RNA viral load increased (VL≤40; 40<VL≤10,000; 10,000<VL≤100,000; and VL>100,000 copies/ml), the occurrence of GI-KS increased significantly ($p<0.01$ for trend in odds, Table 1). Multivariable analysis showed cutaneous KS (OR, 144.8, 95%CI, 58.5–358.2, $p<0.01$) was the only independent clinical factor related to GI-KS.

Predictive clinical factors of GI-KS in patients without GI symptoms

Univariate analysis identified MSM, CD4 count <100 cells/μL, HIV RNA VL≥10,000 copies/mL, no history of HAART, and presence of cutaneous KS as significant clinical factors for the development of GI-KS (Table 2). Multivariable analysis showed cutaneous KS (OR, 128.7, 95%CI, 44.1–376.1, $p<0.01$) was the only independent clinical factor related to GI-KS.

Predictive clinical factors of GI-KS in patients without cutaneous KS

Univariate analysis identified MSM and CD4 count <100 cells/μL as significant clinical factors for the development of GI-KS (Table 2). Multivariable analysis showed MSM (OR, 5.18, 95%CI, 0.79–∞, $p = 0.09$) and CD4 count <100 cells/μL (OR,

Table 2. Predictive clinical factors for GI-KS on uni- and multivariable analysis.

	All (n = 1.027)	Without GI symptoms (n = 659)	Without cutaneous KS (n = 981)
Univariate analysis	**Odds ratio (95%CI)**	**Odds ratio (95%CI)**	**Odds ratio (95%CI)**
Age (years)			
<40	1 (referent)	1 (referent)	1 (referent)
≥40	0.84 (0.41–1.72)	1.00 (0.43–2.34)	0.54 (0.13–21.8)
Sex			
Female	1 (referent)	1 (referent)	1 (referent)
Male	4.33 (0.76–∞)†	3.70 (0.64–∞)†	1.04 (0.16–∞)†
Sexual behavior			
Heterosexual	1 (referent)	1 (referent)	1 (referent)
MSM	7.95 (1.89–33.4)*	5.67 (1.33–24.2)**	5.78 (0.89–∞)†***
CD4 cell count (cells/μL)			
≥100	1 (referent)	1 (referent)	1 (referent)
<100	5.68 (2.75–11.7)*	4.43 (1.99–9.85)*	10.3 (2.06–51.2)*
HIV RNA (copies/mL)			
<10,000	1 (referent)	1 (referent)	1 (referent)
≥10,000	7.40 (3.30–16.6)*	8.52 (3.37–21.6)*	1.49 (0.35–6.29)
History of HAART			
Without	1 (referent)	1 (referent)	1 (referent)
With	0.31 (0.15–0.63)*	0.26 (0.12–0.58)*	0.59 (0.14–2.49)
GI symptoms			
Without	1 (referent)	NA	1 (referent)
With	0.47 (0.20–1.10)***	NA	1.02 (0.24–4.30)
Cutaneous KS			
Without	1 (referent)	1 (referent)	NA
With	144.8 (58.5–358.2)*	128.7 (44.1–376.1)*	NA
Multivariable analysis	Odds ratio (95%CI)	Odds ratio (95%CI)	Odds ratio (95%CI)
MSM			5.18 (0.79–∞)†***
CD4 count <100 cells/μL			9.55 (1.69–97.7)†**
Cutaneous KS	144.8 (58.5–358.2)	128.7 (44.1–376.1)*	NA

†: Analysis by exact logistic regression.
*p<0.01.
**p<0.05.
***p<0.1.
A final model of multivariable analysis was developed by backward selection of factors showing values of p<0.05.
Abbreviations: GI-KS, gastrointestinal Kaposi's sarcoma; MSM, men who have sex with men; HAART, highly active antiretroviral therapy; NA, not applicable.
doi:10.1371/journal.pone.0046967.t002

9.55, 95%CI, 1.69–97.7, p<0.01) were the only independent clinical factors related to GI-KS.

Predictive clinical factors for endoscopic severity of GI-KS

Endoscopic severity was found in the form of bulky tumors (n = 10), ulcerous lesions (n = 11), and multiple lesions (n = 9). Relationships between endoscopic severity of GI-KS and clinical factors are shown in Table 3. In the analysis of GI-KS patients, endoscopic severity in the form of bulky tumors was found to be associated with CD4 cell count <100 cells/μL (p = 0.04). Endoscopic severity in the form of multiple lesions was found to be associated with HIV RNA VL≥10,000 copies/mL (p<0.05). No significant difference was noted in the presence of cutaneous KS between the mild groups and the severe group on endoscopy.

Discussion

Endoscopy is clearly a valuable diagnostic method for identifying GI-KS, but it is not recommended for all HIV-infected patients because of considerations of cost and invasiveness. The present study therefore sought to answer which HIV-infected patients need endoscopy to detect visceral KS.

We found that MSM, low CD4 (<100 cells/μL), high HIV RNA VL (>10,000 copies/mL), no history of HAART, and presence of cutaneous KS were predictive clinical factors for GI-KS on univariate analysis. Our findings are consistent with past studies on HIV-infected patients from Western countries that showed an association between clinical factors and cutaneous KS or visceral KS [2,2,4–7,9–13].

Endoscopy is usually considered to be indicated for GI-KS diagnosis in patients who have GI symptoms [17,18]. However,

Table 3. Relationship between endoscopic severity of GI-KS and clinical factors (n = 33).

Factor	GI-KS with small tumor (n = 23)	GI-KS with bulky tumor (n = 10)	GI-KS without ulcer (n = 22)	GI-KS with ulcer (n = 11)	GI-KS small number (n = 24)	GI-KS large number (n = 9)
Age (yrs) ≥40	60.9%	60.0%	68.2%	45.5%	58.3%	66.7%
Sex (male)	100%	100%	100%	100%	100%	100%
Sexual behavior (MSM)	91.3%†	100%†	95.5%‖	90.9%‖	95.8%¶	88.9%¶
CD4 cell counts <100 cells/μL	52.2%†	90.0%†	59.1%‖	72.2%‖	62.5%¶	66.7%¶
HIV RNA ≥10,000 copies/mL	73.9%†	80.0%†	68.2%‖	90.9%‖	66.7%¶	100%¶
History of HAART	47.8%†	40.0%†	45.5%‖	45.5%‖	45.8%¶	44.4%¶
With GI symptoms	21.7%	20.0%	22.7%	18.2%	25.0%	11.1%
With cutaneous KS	21.7%†	30.0%†	77.3%‖	72.7%‖	79.2%¶	66.7%¶

†: Analysis by chi-square test between GI-KS with small tumor and bulky tumor, MSM (p = 0.34), CD4 (p<0.05), HIV-RNA (p = 0.71), history of HAART (p = 0.68), and presence of cutaneous KS (p = 0.61).
‖: Analysis by chi-square test between GI-KS with small tumor and bulky tumor, MSM (p = 0.61), CD4 (p = 0.44), HIV-RNA (p = 0.15), history of HAART (p = 1.00), and the presence of cutaneous KS (p = 0.77).
¶: Analysis by chi-square test between GI-KS with small tumor and bulky tumor, MSM (p = 0.61), CD4 (p = 0.83), HIV RNA (p<0.05), history of HAART (p = 0.94), and presence of cutaneous KS (p = 0.46).
Abbreviations: GI-KS, gastrointestinal Kaposi's sarcoma; MSM, men who have sex with men; HAART, highly active antiretroviral therapy.
doi:10.1371/journal.pone.0046967.t003

GI-KS can reportedly be detected even in patients without GI symptoms [19,20]. Indeed, we found that 79% of the patients we identified with GI-KS were asymptomatic. Both uni- and multivariable analysis showed that the presence of GI symptoms is not useful in predicting GI-KS. Furthermore, predictive factors for GI-KS were unchanged among patients without GI symptoms.

Previous studies have shown that KS occurs more commonly among MSM with AIDS than among heterosexual individuals with AIDS [2,7,8]. However, the true sexual behavior of a patient might not be able to be ascertainable in interviews, as was attempted in this study. Some MSM patients may well have been included among the unknown cases of non-GI-KS patients, in whom the OR of sexual behavior would be difficult to evaluate.

HAART is known to represent a highly effective treatment for GI-KS, and can improve the immune status of patients [4–6,9–11]. The present study found that a history of long-term administration of HAART reduced the occurrence of GI-KS.

It has previously been shown that patients with KS typically have a low CD4 cell count (<150 cells/μL) and a high HIV RNA VL (>10,000 copies/mL) [9–11]. However, CD4 levels and HIV-RNA VLs have yet to be fully investigated in GI-KS patients. The present study demonstrated that the prevalence of GI-KS tended to increase significantly with low CD4 cell count and with high HIV RNA VL. The presence of GI involvement with KS may vary according to immune status.

KS manifests primarily as a cutaneous disorder, with visceral involvement considered to occur subsequently [2,12]. In this study, the presence of cutaneous KS was found to be closely related to GI-KS on uni- and multivariable analysis. These results suggest that endoscopy may be indicated for patients with cutaneous KS.

It has been reported that GI-KS can occur in the absence of cutaneous disease [20,21]. Thus, we assessed the clinical factors among patients without cutaneous disease. We found that MSM and CD4 count <100 cells/μL were the only independent clinical factors related to GI-KS. Our results represent the first confirmation of this finding evaluated in a case-control study.

We investigated the possibility that HAART administration led to the disappearance of cutaneous KS prior to the diagnosis of GI-KS in patients without cutaneous involvement. In fact, five of eight GI-KS patients without cutaneous KS had a history of HAART. However, the mean duration of the administration was less than 2 months, and it is difficult to imagine that cutaneous KS disappeared from the whole body in such a short period of time. Therefore, it is unlikely that HAART administration had any involvement in the absence of cutaneous KS in these GI-KS patients.

In this study, we assessed endoscopic severity such as tumor bulk, ulceration, and multiple lesions as these may cause obstruction, hemorrhage, and perforation [14,22–26]. We found, for the first time, that CD4 count (<100 cells/μL) or high HIV RNA VL (≥10,000 copies/mL) were key clinical factors to predict severe GI lesions on endoscopy.

A key limitation of this study was the single-center, retrospective nature of the investigation. When considering indications for endoscopy, a randomized controlled study is required to identify whether endoscopy can prevent the development of severe GI complications in HIV-infected patients, particularly among those with a low CD4 count. Second, the number of GI-KS patients was relatively small, especially those without cutaneous KS. The statistical power of the study might thus have been low due to the small number of cases.

Conclusions

To diagnose GI-KS, clinical factors need to be considered before endoscopy is undertaken. Presence of GI symptoms is not useful in predicting GI-KS. The presence of cutaneous KS, MSM sexual behavior, low CD4 count (<100 cells/μL), high HIV RNA VL, and no history of HAART are predictive factors for GI-KS. Even if patients have no cutaneous KS, endoscopy may be suitable for patients with MSM and low CD4 count (<100 cells/μL). Caution should be exercised especially in patients with a low CD4 count (<100 cells/μL) or high HIV RNA VL (≥10,000 copies/mL) as they are more likely to develop severe GI-KS lesions. This diagnostic strategy could facilitate early diagnosis of GI-KS.

Acknowledgments

We are grateful to Hisae Kawashiro (Clinical Research Coordinator) for help with data collection.

Author Contributions

Conceived and designed the experiments: NN SO NU. Performed the experiments: NN TI. Analyzed the data: KT NO TS. Contributed reagents/materials/analysis tools: HY NA. Wrote the paper: NN SO NU JA KT NO.

References

1. Braun M (1982) Classics in oncology. idiopathic multiple pigmented sarcoma of the skin by kaposi. CA: A Cancer Journal for Clinicians 32: 340–347.
2. Beral V, Peterman TA, Berkelman RL, Jaffe HW (1990) Kaposi's sarcoma among persons with AIDS: A sexually transmitted infection? Lancet 335: 123–128.
3. Chang Y, Cesarman E, Pessin MS, Lee F, Culpepper J, et al. (1994) Identification of herpesvirus-like DNA sequences in AIDS-associated kaposi's sarcoma. Science 266: 1865–1869.
4. Buchacz K, Baker RK, Palella FJ Jr, Chmiel JS, Lichtenstein KA, et al. (2010) AIDS-defining opportunistic illnesses in US patients, 1994–2007: A cohort study. AIDS (London, England) 24: 1549–1559.
5. Engels EA, Pfeiffer RM, Goedert JJ, Virgo P, McNeel TS, et al. (2006) Trends in cancer risk among people with AIDS in the united states 1980–2002. AIDS (London, England) 20: 1645–1654.
6. Biggar RJ, Rabkin CS (1996) The epidemiology of AIDS–related neoplasms. Hematology/oncology Clinics of North America 10: 997–1010.
7. Mocroft A, Kirk O, Clumeck N, Gargalianos-Kakolyris P, Trocha H, et al. (2004) The changing pattern of kaposi sarcoma in patients with HIV, 1994–2003: The EuroSIDA study. Cancer 100: 2644–2654.
8. Beral V, Bull D, Darby S, Weller I, Carne C, et al. (1992) Risk of kaposi's sarcoma and sexual practices associated with faecal contact in homosexual or bisexual men with AIDS. Lancet 339: 632–635.
9. Lodi S, Guiguet M, Costagliola D, Fisher M, de Luca A, et al. (2010) Kaposi sarcoma incidence and survival among HIV-infected homosexual men after HIV seroconversion. Journal of the National Cancer Institute 102: 784–792.
10. Gallafent JH, Buskin SE, De Turk PB, Aboulafia DM (2005) Profile of patients with kaposi's sarcoma in the era of highly active antiretroviral therapy. Journal of Clinical Oncology: Official Journal of the American Society of Clinical Oncology 23: 1253–1260.
11. Stebbing J, Sanitt A, Nelson M, Powles T, Gazzard B, et al. (2006) A prognostic index for AIDS-associated kaposi's sarcoma in the era of highly active antiretroviral therapy. Lancet 367: 1495–1502.
12. Dezube BJ (1996) Clinical presentation and natural history of AIDS–related kaposi's sarcoma. Hematology/oncology Clinics of North America 10: 1023–1029.
13. Ngendahayo P, Mets T, Bugingo G, Parkin DM (1989) [Kaposi's sarcoma in rwanda: Clinico-pathological and epidemiological aspects]. Bulletin Du Cancer 76: 383–394.
14. Danzig JB, Brandt LJ, Reinus JF, Klein RS (1991) Gastrointestinal malignancy in patients with AIDS. The American Journal of Gastroenterology 86: 715–718.
15. Laine L, Amerian J, Rarick M, Harb M, Gill PS (1990) The response of symptomatic gastrointestinal kaposi's sarcoma to chemotherapy: A prospective evaluation using an endoscopic method of disease quantification. The American Journal of Gastroenterology 85: 959–961.
16. Ioachim HL, Adsay V, Giancotti FR, Dorsett B, Melamed J (1995) Kaposi's sarcoma of internal organs. A multiparameter study of 86 cases. Cancer 75: 1376–1385.
17. Krown SE, Testa MA, Huang J (1997) AIDS-related kaposi's sarcoma: Prospective validation of the AIDS clinical trials group staging classification. AIDS clinical trials group oncology committee. Journal of Clinical Oncology: Official Journal of the American Society of Clinical Oncology 15: 3085–3092.
18. Nasti G, Talamini R, Antinori A, Martellotta F, Jacchetti G, et al. (2003) AIDS-related kaposi's sarcoma: Evaluation of potential new prognostic factors and assessment of the AIDS clinical trial group staging system in the haart era–the italian cooperative group on AIDS and tumors and the italian cohort of patients naive from antiretrovirals. Journal of Clinical Oncology: Official Journal of the American Society of Clinical Oncology 21: 2876–2882.
19. Friedman SL, Wright TL, Altman DF (1985) Gastrointestinal kaposi's sarcoma in patients with acquired immunodeficiency syndrome. endoscopic and autopsy findings. Gastroenterology 89: 102–108.
20. Kahl P, Buettner R, Friedrichs N, Merkelbach-Bruse S, Wenzel J, et al. (2007) Kaposi's sarcoma of the gastrointestinal tract: Report of two cases and review of the literature. Pathology, Research and Practice 203: 227–231.
21. Barrison IG, Foster S, Harris JW, Pinching AJ, Walker JG (1988) Upper gastrointestinal kaposi's sarcoma in patients positive for HIV antibody without cutaneous disease. British Medical Journal (Clinical Research Ed.) 296: 92–93.
22. Yoshida EM, Chan NH, Chan-Yan C, Baird RM (1997) Perforation of the jejunum secondary to AIDS-related gastrointestinal kaposi's sarcoma. Canadian Journal of Gastroenterology = Journal Canadien De Gastroenterologie 11: 38–40.
23. Nagata N, Yazaki H, Oka S (2011) Kaposi's sarcoma presenting as a bulky tumor mass of the colon. Clin Gastroenterol Hepatol 9: A22.
24. Lingenfelser T, Daiss W, Overkamp D, Weber P (1994) Successful mono-chemotherapy of extensive gastrointestinal kaposi's sarcoma with bowel obstruction in acquired immunodeficiency syndrome. Zeitschrift Fur Gastroenterologie 32: 688–690.
25. Carratala J, Lacasa JM, Mascaro J, Torras JT (1992) AIDS presenting as duodenal perforation due to kaposi's sarcoma. AIDS (London, England) 6: 241–242.
26. Ravalli S, Vincent RA, Beaton H (1990) Primary kaposi's sarcoma of the gastrointestinal tract presenting as acute appendicitis. The American Journal of Gastroenterology 85: 772–773.
27. Weprin L, Zollinger R, Clausen K, Thomas FB (1982) Kaposi's sarcoma: Endoscopic observations of gastric and colon involvement. Journal of Clinical Gastroenterology 4: 357–360.
28. Kahn HJ, Bailey D, Marks A (2002) Monoclonal antibody D2–40, a new marker of lymphatic endothelium, reacts with kaposi's sarcoma and a subset of angiosarcomas. Modern Pathology: An Official Journal of the United States and Canadian Academy of Pathology, Inc 15: 434–440.
29. Rosado FG, Itani DM, Coffin CM, Cates JM (2012) Utility of immunohistochemical staining with FLI1, D2–40, CD31, and CD34 in the diagnosis of acquired immunodeficiency syndrome-related and non-acquired immunodeficiency syndrome-related kaposi sarcoma. Archives of Pathology & Laboratory Medicine 136: 301–304.

frontiers in
MICROBIOLOGY

REVIEW ARTICLE
published: 25 August 2011
doi: 10.3389/fmicb.2011.00175

Pathology of Kaposi's sarcoma-associated herpesvirus infection

*Hitomi Fukumoto[1,2], Takayuki Kanno[1], Hideki Hasegawa[1] and Harutaka Katano[1]**

[1] Department of Pathology, National Institute of Infectious Diseases, Tokyo, Japan
[2] Military Medicine Research Unit, Japan Ground Self Defense Force, Tokyo, Japan

Edited by:
Keiji Ueda, Osaka University Graduate School of Medicine, Japan

Reviewed by:
Hiroki Isomura, Aichi Cancer Center Research Institute, Japan
Keiji Ueda, Osaka University Graduate School of Medicine, Japan

***Correspondence:**
Harutaka Katano, Department of Pathology, National Institute of Infectious Diseases, 1-23-1 Toyama, Shinjuku-ku, Tokyo 162-8640, Japan.
e-mail: katano@nih.go.jp

Kaposi's sarcoma-associated herpesvirus (KSHV; human herpesvirus 8) is a human herpesvirus, classified as a gamma-herpesvirus. KSHV is detected in Kaposi's sarcoma (KS), primary effusion lymphoma (PEL), and some cases of multicentric Castleman's disease (MCD). Similar to other herpes viruses, there are two phases of infection, latent and lytic. In KSHV-associated malignancies such as KS and PEL, KSHV latently infects almost all tumor cells. Quantitative PCR analysis revealed that each tumor cell contains one copy of KSHV in KS lesions. The oncogenesis by KSHV has remained unclear. Latency-associated nuclear antigen (LANA)-1 plays an important role in the pathogenesis of KSHV-associated malignancies through inhibition of apoptosis and maintenance of latency. Because all KSHV-infected cells express LANA-1, LANA-1 immunohistochemistry is a useful tool for diagnosis of KSHV infection. KSHV encodes some homologs of cellular proteins including cell-cycle regulators, cytokines, and chemokines, such as cyclin D, G-protein-coupled protein, interleukin-6, and macrophage inflammatory protein-1 and -2. These viral proteins mimic or disrupt host cytokine signals, resulting in microenvironments amenable to tumor growth. Lytic infection is frequently seen in MCD tissues, suggesting a different pathogenesis from KS and lymphoma.

Keywords: Kaposi's sarcoma-associated herpesvirus, HHV-8, latency-associated nuclear antigen, LANA-1, primary effusion lymphoma

INTRODUCTION

The 1994 discovery of Kaposi's sarcoma-associated herpesvirus (KSHV, human herpesvirus 8, HHV-8) in Kaposi's sarcoma (KS) tissues had a huge impact, not only in the field of virology, but also on bioscience generally (Chang et al., 1994; Ganem, 2005). Before the discovery of KSHV, almost all viruses had been identified using conventional virus isolation methods with cell cultures. DNA fragments of KSHV were identified in KS tissues by representational difference analysis, which is a subtraction PCR-based method to purify restriction-endonuclease-digested fragments present in one population of DNA fragments but not in others (Chang et al., 1994). Thus, KSHV is the first virus whose fragments were identified directly by the PCR method before any cell culture methods. In 1996, KSHV-infected cell lines were established, based on the fragments' DNA sequences (Renne et al., 1996b). Herpesvirus-like particles of this virus were found in lymphoma cells by electron microscopic analysis. Finally, KSHV's full DNA sequence was determined (Russo et al., 1996). Over the 15-years since the discovery of KSHV, it has been established as a tumor virus (Ganem, 2005). Some KSHV-encoded genes are homologous to oncogenes or cell-cycle-associated genes (Russo et al., 1996); some are transformational genes, able to transform human cells (Gao et al., 1997; Bais et al., 1998; Lee et al., 1998; Muralidhar et al., 1998). However, expression of KSHV-encoded genes is severely restricted; only a few viral genes are expressed in KSHV-infected cells. The KSHV-encoded latency-associated nuclear antigen 1 (LANA-1) is the only protein whose expression is stably detected by immunohistochemistry in KSHV-infected cells (Dupin et al., 1999; Katano et al., 2000b). LANA-1 is a multifunctional protein, but has no full transforming activity. In comparison, Epstein–Barr virus (EBV) encodes a full oncogenic protein, latent membrane protein-1 (LMP1), which is expressed in a subset of EBV-latently infected cells (Cohen, 2000). Thus, KSHV oncogenesis is not simple. Many KSHV-encoded non-transforming proteins apparently collaborate to establish and maintain oncogenesis in KSHV-infected cells. In this review, the pathological aspects of KSHV infection and KSHV-associated diseases are summarized.

VIRUS AND ITS GENE EXPRESSION

Usually, viral particles are not observed in KS samples by electron microscope because of the small number of KSHV copies. However, they can be seen in primary effusion lymphoma (PEL) cell lines stimulated by 12-*O*-tetradecanoylphorbol-13-acetate (TPA). A complete viral particle of KSHV, consisting of a capsid and an envelope (Renne et al., 1996b; Said et al., 1996, 1997; Orenstein et al., 1997; Ohtsuki et al., 1999), is 150–200 nm in diameter, which is similar to other human herpes viruses and indistinguishable from other herpes viruses. The unenveloped capsid is produced in the host nucleus and is 100 nm in diameter. It contains a central DNA core, which appears to have a high electron density. The envelope is derived from the inner nuclear membrane, as viral particles bud into the cytoplasm from the nucleus. The tegument protein fills the space between the nucleocapsid and envelope. This feature

of viral particles is apparently quite similar among herpes viruses, but related structures forming in infected cells seem to depend on the type of virus.

The KSHV genome consists of linear, double-stranded DNA of about 170 kbp (Renne et al., 1996a; Russo et al., 1996). The KSHV genome consists of a long unique region (LUR) and a terminal repeat (TR) at both termini, which resembles the herpes virus saimiri structure (Russo et al., 1996). The TRs consist of 801-bp direct repeat units having 84.5% GC content. The number of repeats in TRs may vary. The LUR is 140.5 kbp and has 53.5% GC content. KSHV encodes more than 80 viral proteins on LUR. KSHV also encodes 17 microRNAs (miRNAs), which are derived by processing from 12 pre-miRNAs (Cai et al., 2005). Kinetics of KSHV-encoded genes were mainly investigated in KSHV-infected PEL cell lines stimulated with phorbol ester such as TPA (Sun et al., 1999). Like other herpesviruses, viral genes were categorized into lytic and latent genes, and also into immediate-early (IE), early (E), and late (L) genes based on their expressions. The function of each KSHV-encoded gene was summarized in the **Table 1**. Open reading frame 50 (*ORF50*) is an IE gene that is a homolog of *Rta*, a transcriptional activator encoded by EBV (Lukac et al., 1999; Seaman et al., 1999; Sun et al., 1999; Zhu et al., 1999). Transcription of *ORF50* results in its expression within 4 h after stimulation by TPA. This expression could not be blocked by phosphonoacetic acid (a herpesvirus-DNA polymerase inhibitor) nor cycloheximide (a protein synthesis inhibitor). Transfection of *ORF50* to KSHV-infected cells resulted in the activation of lytic gene expression (Lukac et al., 1999). Thus, ORF50 protein is a lytic switch protein. Expression of ORF50 protein is required for expression of many KSHV-encoded lytic genes such as *K3*, and *K5* (homologs of the IE gene of *BHV-4*), viral interleukin-6 (*vIL-6*), viral macrophage inflammatory proteins (*vMIPs*), polyadenylated nuclear RNA (*PAN*), *vBcl-2*, *K12*, viral G-protein-coupled receptor (*vGPCR*), viral dihydrofolate reductase (*vDHFR*), DNA replication factors, and thymidylate synthase (Sarid et al., 1998). ORF50 protein also induces expression of K8 (K-bZIP, a positional homolog of EBV BZLF1) protein, an early protein. K8 protein plays a role as transactivation repressor for ORF50 protein, leading to a negative autoregulation system during lytic infection (Liao et al., 2003). Late genes, including tegument proteins, and virion-associated protein are then expressed (**Table 1**).

Latent infection is predominant in KSHV infection. KSHV codes a latency-associated gene cluster including *ORF73* (*LANA-1*, *LNA*, or *LNA-1*), v-cyclin (*ORF72*), viral FLICE-inhibitory protein (*K13*, *v-FLIP*), Kaposin (*K12*), and viral-encoded miRNAs. LANA-1 is always detected as a dot-like staining pattern in KSHV-infected cells by immunohistochemistry. KSHV-encoded 17 miRNAs, which are derived by processing from 12 pre-miRNAs, are expressed during viral latency (Cai et al., 2005; Samols et al., 2005).

Table 1 | Kaposi's sarcoma-associated herpesvirus genes and their functions.

Gene	Phase	Functions
LANA-1	Latent	Always express in KSHV-infected cells Maintain and replicate viral genome during mitotic division by holding KSHV episome at chromosome Bind to p53 and inhibit p53-dependent apoptosis Bind to Rb and inhibit Rb-E2F pathway Bind to GSK-3β, and induce accumulation of β-catenin
LANA-2	Latent	Expressed in only PEL cells, not in KS cells Homolog of IRF Inhibit p53-dependent apoptosis
Kaposin	Latent	Kaposin A: transformation activity? Kaposin B, C: associate with cytokine expression as adaptor protein of MAP kinase-associated protein kinase 2 (MK2)
v-cyclin	Latent	Homolog of cyclin D1 Inhibit P27Kip1, and induce cell-cycle to S-phase
v-FLIP	Latent	Anti-apoptosis
ORF50 (RTA)	Lytic (IE)	Lytic switch protein Transactivator for K8
K1	Lytic	Transformation activity
K8	Lytic (early)	Transcriptional repressor for RTA
K3, K5	Lytic (IE/early)	Down-regulation of MHC class I expression
vIL-6	Lytic (early)	Induce VEGF expression Induce constitutional activation of Stat3 Disrupt anti-viral function by IFN-α
vIRF-1	Lytic (early)	Disrupt IFN signal Transformation activity?
vMIPs	Lytic (early)	Bind to chemokine receptors and induce angiogenesis
vBcl-2	Lytic (early)	Inhibit apoptosis
vGPCR	Lytic (early)	Transformation activity Bind to IL-8 Induce VEGF expression
K15	Lytic	Bind to TRAF family, and induction of NF-κB activation

KSHV ONCOGENESIS

The first evidence of transformation activity by KSHV came from a report describing that human umbilical vein endothelial cells (HUVEC) were transformed and immortalized by KSHV infection *in vitro* (Flore et al., 1998). However, such KSHV-infected HUVEC did not express any KSHV gene, and the immortalization by KSHV infection was not confirmed by any other groups (Gao et al., 2003; Tang et al., 2003). KSHV efficiently infects primary cultures of human endothelial cells *in vitro* (Sakurada et al., 2001; Gao et al., 2003). KSHV-infected cells express LANA-1 within several hours after infection. One week after infection, a large portion of culture cells will be infected by KSHV and expressing LANA-1. Interestingly, expression of any lytic proteins encoded by KSHV is not observed at that time. Latent infection is dominant in KSHV-infected cells *in vivo* and *in vitro*. Although some KSHV-encoded proteins such as K1 and vGPCR

are shown to have a transformation activity on mammalian cells, these transforming proteins are not usually expressed in KSHV-infected cells (Bais et al., 1998; Lee et al., 1998; Montaner et al., 2003). However, LANA-1, a major KSHV-encoded latency protein, is always expressed in KSHV-infected cells both *in vivo* and *in vitro* (Dupin et al., 1999; Katano et al., 1999b; Kellam et al., 1999). Moreover, latency is maintained during the presence of KSHV in the cells. Thus, LANA-1 clearly plays an important role in the pathogenesis of KSHV infection, and has been shown to be a multifunctional protein. Probably the most important role of LANA-1 is to establish and maintain the latency in KSHV-infected cells by tethering KSHV DNA to host chromosomes (Ballestas et al., 1999). LANA-1 binds directly to TR sequences of the KSHV genome, and recruits it to the host chromosome (**Figure 1E**). The DNA of KSHV is replicated during host cell divisions using host DNA replicative machinery (Sakakibara et al., 2004). Thus, daughter cells inherit KSHV genome without any virus particle. LANA-1 is also associated with signal transduction in KSHV-infected cells. LANA-1 binds directly to p53, a major tumor repressor and anti-apoptotic factor (Friborg et al., 1999). Viral infection usually induces p53 expression and p53-dependent apoptosis as self-defense system. Direct interaction with p53 by LANA-1 results in inhibition of p53-dependent apoptosis in KSHV-infected cells. Moreover, LANA-1 stabilizes β-catenin by binding to the negative regulator GSK-3β, promoting cell-cycle induction by nuclear accumulation of GSK-3β (Fujimuro et al., 2003). Thus, LANA-1 plays a central role in the pathogenesis of KSHV infection, but LANA-1 itself does not have any full transformation activity. Many other factors besides LANA-1 are required to establish KSHV oncogenesis.

Another important factor in KSHV oncogenesis is that KSHV encodes many homologs of human genes. The viral genes of human gene homologs cooperate to establish suitable growth conditions for KSHV-infected cells. Among them, vIL-6 is the most important factor for KSHV pathogenesis. vIL-6 induces angiogenesis by vascular endothelial cell growth factor (VEGF) expression (Aoki et al., 1999), and stimulates the constitutive Jak-Stat pathway through the Stat3 signal, resulting in cell growth (Aoki et al., 2003). In addition, vIL-6 represses the anti-viral function of interferon by binding to a subunit of human IL-6 receptor and suppressing p21 expression (Chatterjee et al., 2002). KSHV-encoded vMIP-1, vMIP-2, vBcl-2, vIRF-1, v-cyclin D, and v-FLIP mimic their human homologs, and work sometimes as inhibitors and sometimes as mimics, resulting in growth of KSHV-infected cells. Because almost all these mimics are lytic proteins, their expression is not usually observed. However, some cytokines may induce their expression independently to lytic and latent infection as necessary. Thus, KSHV oncogenesis is established by cooperation of many viral proteins such as LANA-1 and by the mimic, rather than the primary functions of oncogenetic transformation genes encoded by the virus.

Recently, miRNA has been shown to affect tumor biology. Several KSHV miRNAs were shown to modulate host gene expression, suggesting some roles for miRNA in the pathogenesis of KSHV-induced malignancies. Thrombospondin 1, a potent inhibitor of angiogenesis that is reportedly downregulated in KS lesions, is targeted by multiple miRNAs (Samols et al., 2007). The target of miR-K5 is Bcl2-associated factor BCLAF1, which promote apoptosis (Lei et al., 2010). MiR-K1 targets IκBα, an inhibitor of NF-κB. NF-κB inhibits the activation of lytic viral promoters. By activating NF-κB, miR-K1 suppresses viral lytic replication, maintaining latent infection (Ziegelbauer et al., 2009). So far, miRNAs' roles in viral infection and replication remain unclear.

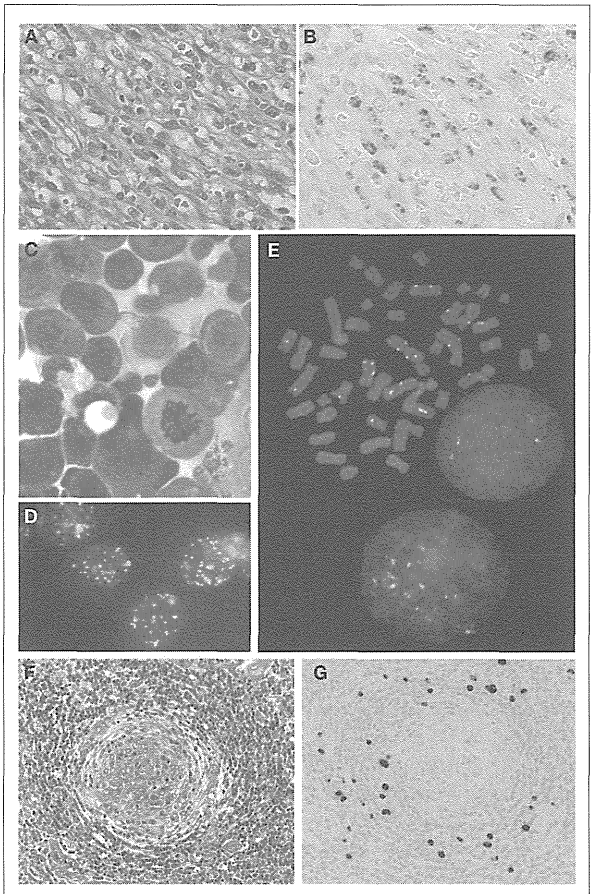

FIGURE 1 | Histological analysis on KSHV-associated diseases. (A) Nodular stage of KS; HE staining. **(B)** LANA-1 immunohistochemistry of KS. **(C)** Giemsa staining of PEL. **(D)** LANA-1 immunofluorescence staining in mitosis of PEL cells. **(E)** LANA-1 immunostaining of mitosis of PEL cell line, TY-1. Yellow signals indicate LANA-1. Red is counter staining of chromosome. **(F)** HE staining of MCD. **(G)** LANA-1 immunohistochemistry of MCD.

EPIDEMIOLOGY

Serological studies have revealed that KSHV-infected individuals are found all over the world. Serum antibody to KSHV is detected with ELISA using lysate of KSHV viral particles or recombinant viral proteins as antigens, or immunofluorescence assay using KSHV-infected cells. The seroprevalence of KSHV infection differs among regions/countries. Among the general population, KSHV seropositivity is less than 10% in northern Europe, America, and Asia, 10–30% in the Mediterranean region, and more than